Improvement and Validation of an Analytical Code for Ship Collisions Based on Super-Element Method

Bayram Ozdogan

Master Thesis

presented in partial fulfillment
of the requirements for the double degree:
“Advanced Master in Naval Architecture” conferred by University of Liege
"Master of Sciences in Applied Mechanics, specialization in Hydrodynamics, Energetics and Propulsion” conferred by Ecole Centrale de Nantes

developed at L'Institut Catholique d'Arts et Métiers, Nantes Campus
in the framework of the

“EMSHIP”
Erasmus Mundus Master Course
in “Integrated Advanced Ship Design”

EMJMD 159652 – Grant Agreement 2015-1687

Supervisor: Prof. Hervé Le Sourne, L’Institut Catholique d’Arts et Métiers

Ing. Stéphane Paboeuf, Bureau Veritas, Nantes

Reviewer: Prof. Philippe Rigo, University of Liège.

Nantes, January 2018

Blank page

Declaration of Authorship

I, Bayram Ozdogan declare that this thesis and the work presented in it are my own and has been generated by me as the result of my own original research.

Improvement and Validation of an Analytical Code for Ship Collisions Based on Super-Element Method

I confirm that:

1. This work was done wholly or mainly while in candidature for a research degree at this University;

2. Where any part of this thesis has previously been submitted for a degree or any other qualification at this University or any other institution, this has been clearly stated;

3. Where I have consulted the published work of others, this is always clearly attributed;

4. Where I have quoted from the work of others, the source is always given. With the exception of such quotations, this thesis is entirely my own work;

5. I have acknowledged all main sources of help;

6. Where the thesis is based on work done by myself jointly with others, I have made clear exactly what was done by others and what I have contributed myself;

7. None of this work has been published before submission;

8. I cede copyright of the thesis in favour of Institut Catholique d'Art et Métiers, Nantes Campus.

Signed:

Date: 26.01.2018

Blank page

CONTENTS

LIST OF FIGURES

LIST OF TABLES

ABBREVIATIONS

3D	: 3 Dimensions
A.D.N.	: European Agreement concerning the International Carriage of Dangerous Goods by Inland Waterways
BV	: Bureau Veritas
CCNR	: Central Commission for the Navigation of the Rhine
DOF	: Degree of Freedom
DTU	: Technical University of Denmark
EMSHIP	: Erasmus Mundus Master Course in Advanced Ship Design
EU	: European Union
FE	: Finite Element
FEA	: Finite Element Analysis
FEM	: Finite Element Method
FEMB	: Finite Element Model Builder
GUI	: Graphical User Interface
ICAM	: l'Institut Catholique d'Arts et Métiers
IMO	: International Maritime Organization
ITOPF	: International Tanker Owner's Pollution Federation
MARPOL	: International Convention for the Prevention of Pollution from Ships
MCOL	: Mitsubishi Collision
MIT	: Massachusetts Institute of Technology
OPA	: Oil Pollution Act
P.R.R.	: Post Rupture Resistance
SE	: Super-Element
SEM	: Super-Element Method
SHARP	: Ship Hazardous Aggression Research Program
SIMCOL	: Simplified Collision Model
SNAME	: Society of Naval Architects and Marine Engineers
SSC	: Ship Structure Committee
UNECE	: United Nations Economic Commission for Europe

Blank page

ABSTRACT

In recent years, inland navigation is increasing its contribution to transportation sector. Besides, with the increasing construction technology and knowledge about routes, it is possible to build bigger vessels. As a consequence, possible amount of the spillage in case of cargo tank rupture is increasing as well. Day by day new rules and precautions are taking effect in order to prevent that. However it is impossible to decrease the possibility of an accident to zero.

Nonetheless especially about vessels which are carrying dangerous goods, possibility of cargo spillage must be kept in minimum level. ADN Regulations guide the construction of inland waterway vessels. ADN Regulations recommend to determine the probability of tank rupture in a collision event by finite element analysis which is time consuming and indigent to expertise. On the other hand thanks to cooperation of BV and ICAM, an analytical tool which is called SHARP was developed in order to determine the tank rupture probability.

In a previous thesis which was studied by Sone Oo, SHARP was compared to non-linear finite element explicit code, LS-Dyna in the scope of ADN Regulations. In this paper, some of the major deficiencies which were revealed by former study will be studied and the analytical code of SHARP will be improved in consideration of results.

Blank page

1. INTRODUCTION

1.1. Background and Motivation

In order to see the motivation of this study, it will be a beneficial way to check close historical statistics about ship to ship collisions and groundings. Such kind of undesired events cause environmental disasters and huge economic loses. The costs of these spills are very high as well. UNCTAD (p. 17) estimates that the cost of cleaning up spilled oil in a European port is about $7 000 for each cubic meters of oil; chemical spills, of course, are much more expensive to clean up as the massive oil spills like the Exxon Valdes (OECD, 1993). The environmental disaster caused by Exxon Valdez oil tanker in the coast of Alaska in 1989 is considered the largest oil spill catastrophe, with the destruction of hundreds of kilometres of ecosystems in a virgin coastline of Alaska (Calle, Alves, 2015). In that disaster 10.8 millions of gallons of oil spilled into the ocean.

In addition to this, it must be remembered that the spilled good is not oil always. According to Eurostats; explosive substances, gases, flammable liquids and solids, self-reactive substances and solid desensitized explosives are being carried by inland navigation as well (Eurostat, 2016). The consequences of that goods will be much more vexatious.

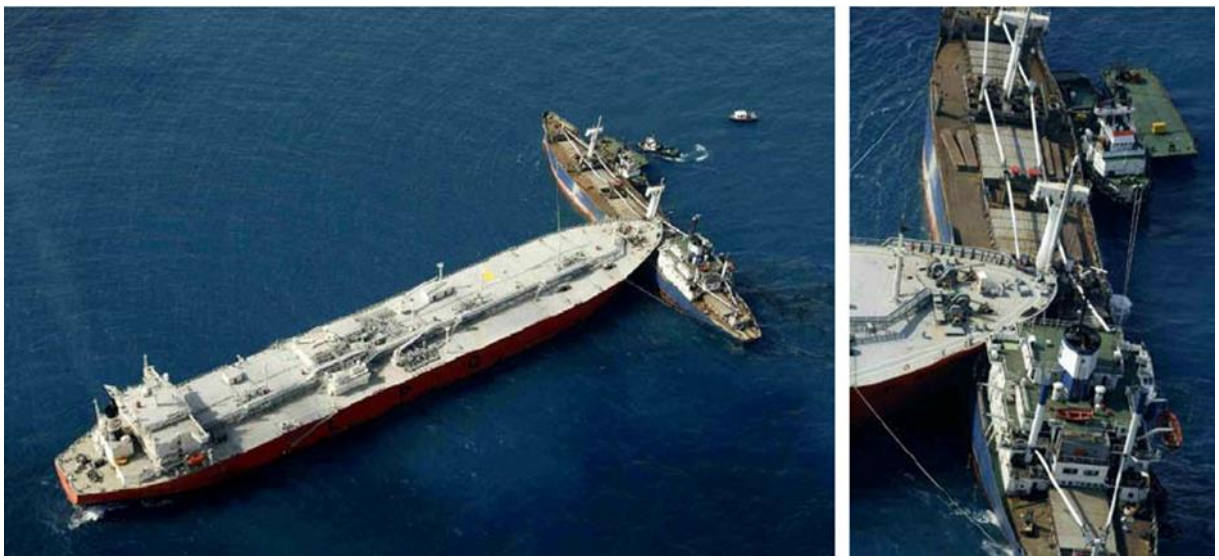

Figure 1 - Ship collision of Gas Roman and Springok near Singapore coast occurred in 2003

The spillage can be caused by different type of undesired events. According to Youssef, Kim and Paik groundings and collisions are dominating (Youssef, Kim and Paik, 2014). The figure below shows the type of the accidents occured between 1970 and 2004 in which spilled more than 700 tonnes of oil.

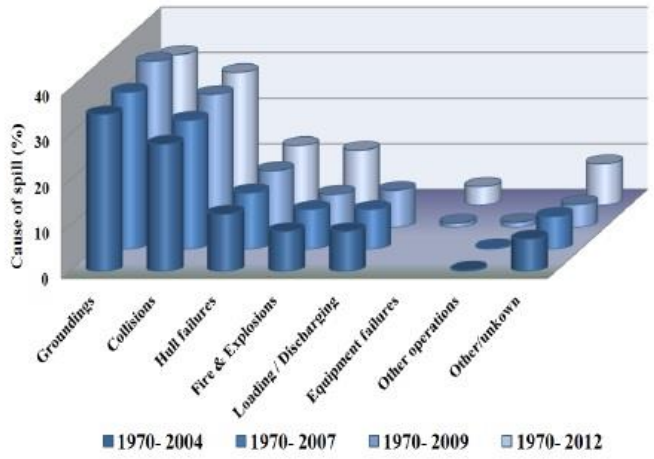

Figure 2 - Accident Types from 1970 – 2004

Besides; tankers, bulk carriers, cargo vessels and container ships are dominating the most striking vessel types (Youssef, Kim and Paik, 2014). Following figure shows the type of the vessels which are involved in an accident.

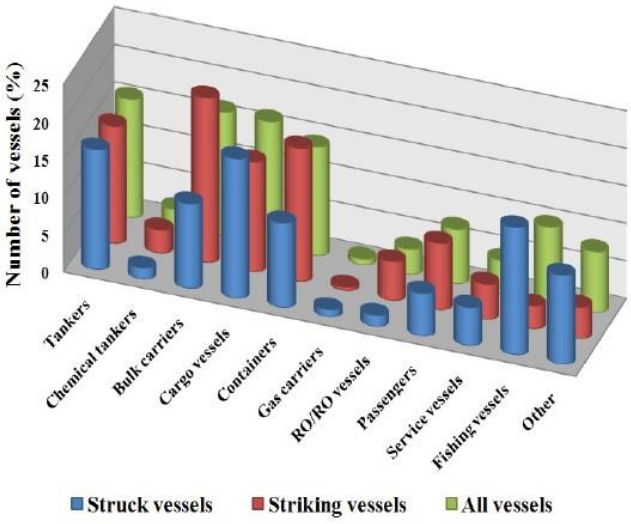

Figure 3 - Ship Types Involved in an Accident

1.2. ADN Regulations

ADN is an European Agreement concerning the International Carriage of Dangerous Goods by Inland Waterways. It has been created at GENEVA on 26 May 2000 by United Nations Economic Commission for Europe (UNECE) and the Central Commission for the Navigation of the Rhine (CCNR) entered into force on 28 February 2008 (United Nations, 2017). The goal of the regulations can be generalized under three main subjects;

a) increasing the safety of international carriage of dangerous goods by inland waterways;
b) contributing effectively to the protection of environment, by preventing any pollution resulting from accidents or incidents during such carriage;
c) facilitating transport operations and promoting international trade, (United Nations,2017).

According to ADN, dangerous goods can be divided into 9 divisions;

- Class 1 Explosives
- Class 2 Gases
- Class 3 Flammable liquids
- Class 4 Flammable solids; substances liable to spontaneous combustion; substances which on contact with water, emit flammable gases
- Class 5 Oxidizing substances and organic peroxides
- Class 6 Toxic and infectious substances
- Class 7 Radioactive materials
- Class 8 Corrosive substances
- Class 9 Miscellaneous dangerous substances and articles, including environmentally hazardous substances

And according to ADN following goods are allowed to be carried by inland waterways;

- Class 2 Gases
- Class 3 Flammable liquids
- Class 5.1 Oxidizing substances
- Class 6 Toxic substances
- Class 8 Corrosive substances

ADN classifies the tank vessels according to goods they carry as Type G, Type C and Type N tank vessels.

Type G vessels; are the vessels which have pressurized gas tanks.
Type C vessels; are the vessels which carry chemical goods
Type N vessels; N refers normal loads. This type of vessel carries liquid dangerous goods.
In future thesis work, Type C vessels will be studied.

According to ADN, following formula determines the risk of cargo tank rupture during a ship collision;

$$R = P.C \tag{1}$$

Where;

R : risk [m2];

P : probability of cargo tank rupture; and

C : consequence (measure of damage) of cargo tank rupture [m2].

For ADN, there are 13 steps to calculate *'P'* which stands for probability of cargo tank rupture. Those steps will not be explained in this paper. But main features of that method which interests this study are;

- Right angle collision scenarios with V-shape striking bow will be considered.
- Struck ship will be at rest and striking ship will surge with 10 m/s velocity.
- Striking bow will be assumed rigid while struck ship is deformable.

1.3. Main Objective of the Thesis

This thesis will focus on the deficiencies in SHARP software. Previous studies have shown that SHARP is an effective tool for analysing ship collisions. However, it contains some inconsistencies. The theory which SHARP is using and mentioned deficiencies will be explained in following parts of this study. In present thesis, the reason behind these deficiencies will be researched and possible solutions will be proposed.

2. EXISTING METHODS FOR SHIP COLLISSION ANALYSIS

Ship collusions have been studied for several decades. Basically when ships are moving, they acquire kinetic energy and during the collision event, this energy causes structural deformations and ruptures until the velocities (considering their directions as well) of both vessels are equal.

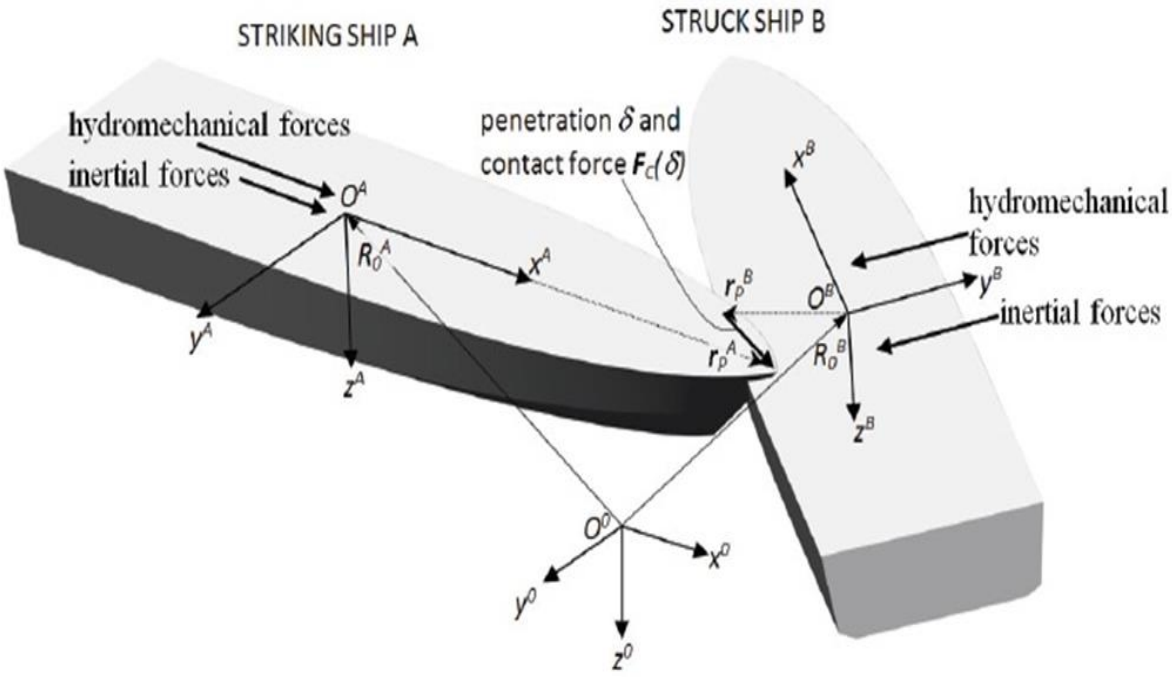

Figure 4 - Definition of Collision Dynamics and Kinematics

In order to study this behaviour, different methods and combinations of them have been used. These methods can be generally divided as in the following list;

- Internal mechanics sub-models
- External dynamics sub-models
- Coupled approach of internal and external mechanics sub-models
- Finite element modelling
- Experimental test of scaled-model
- Super-element Method

2.1. Internal Structural Mechanics

This collision method includes the internal mechanics and structural response of the stuck ship and possibly the striking bow during collision (Chen, 2000). The encounter force in a ship collision accident is dependent to the deformation resistance or affected volume of steel structure elements. This method is based on an empirical formula which was developed by Minorsky (1959) to estimate the deformation energy of a ship collision accident. His formula was derived from 26 actual ship accidents. His formula relates the absorbed energy with affected volume:

$$\Delta KE = (47.1 \pm 8.8)\, RT + 28.4 \qquad (2)$$

Where;

ΔKE [MJ]: Absorbed energy by the struck ship

RT [m3]: Affected volume of steel structure of the struck ship

Besides Minorsky has systematically investigated collisions between ships for the design of American nuclear powered ship N/S Savannah. The main idea of his study was that a linear correlation exists between the deformed steel volume and absorbed energy (Saul and Svensson, 1982).

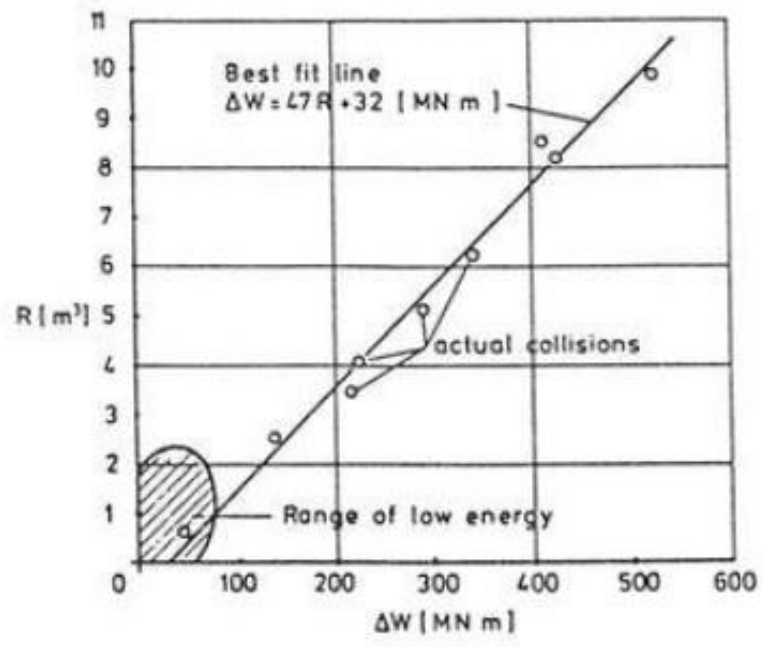

Figure 5 - Relation Between Absorbed Energy and Deformed Steel Volume

Minorsky's formulation was studied and extended several times. Woisin (1979) improved the formulation in order to include low-energy collisions. Vaughan (1978) established new formulation to relate the energy with damaged material volume including the area of tearing in his formulation. Suzuki et al. (2000) tested Minorsky's model by using a simplified rigid plastic analysis of the collision between two tanker vessels. One of the vessels was ten times bigger than the other one and results of that study demonstrated that Minorsky's estimation was incorrect when one of the vessels' stucture are much stronger than the other one (Calle and Alves, 2011).

2.2. External Ship Dynamics

This model deals with both principal charachteristics of the colliding ships with their global motion and the water around the vessels. There are one, two and three degreees of freedom approaches. The simplest one is one-dimesional approach which was proposed by Minorsky (1959).

DAMAGE is a software which was delevoped by Wierzbicki and Simonsen in MIT and allows to analyze collision dynamics in two degrees of freedom. In Minorsky's method, both vessels have one degree of freedom, for striking ship it is surge and for the struck vessel it is sway. In DAMAGE, struck ship has also DOF towards the yawing direction.

For three degrees of freedom approaches Crake, Hutchison and Zhang have more sharp and realistic models.

2.2.1. One Degree of Freedom Approach

Ship collision studies started with nuclear material transportation. In the beginning, fundamental interest was 'worse case'. For this concern, an absolute plastic 90° collision when struck ship at rest condition was defined as 'worse case' (Chen, 2000). Minorsky's approach makes three assumptions;

- Rotations are neglected.
- Collision is totally inelastic.
- The kinetic energy along the struck ship's centerline is neglected.

$$\Delta KE = \frac{M_{B+}\, M_A}{2\, M_A + 1.43\, M_B}\ (V_B sin\varphi)^2 \qquad (3)$$

Where;

ΔKE: Absorbed kinetic energy during collision

M_A: Mass of the struck ship

M_B: Mass of the striking ship

V_B : Initial velocity of the striking ship in Y direction

φ: Collision angle

2.2.2. Two Degrees of Freedom Approach

MIT's DAMAGE sofware allows to consider the yaw for struck ship. The striking ship has only one degree of freedom and the struck ship has zero initial velocity again.

$$\Delta KE = \frac{1}{2} M_{1y} v_1^{a^2} + \frac{1}{2} M_{2x} v_2^{a^2} + \frac{1}{2} I_{1z} w_1^{a^2} - \frac{1}{2} M_{2x} v_2^2 \qquad (4)$$

ΔKE : Absorbed kinetic energy during collision

M_{1y}: Virtual mass of the struck ship including added mass in the sway direction;

M_{2x} : Virtual mass of the striking ship including added mass in the surge direction;

I_{1z} : Virtual moment of inertia in yaw of the struck ship including yaw added mass;

v_1^a : Final velocity of struck ship in the sway direction;

w_1^a : Final angular velocity of struck ship;

v_2 : Initial velocity of striking ship;

v_2^a : Final velocity of striking ship in the sway direction of the struck ship;

This software is not effective to use in different angles than right angle or when struck ship has an initial velocity (Chen,2000).

2.2.3. Three Degrees of Freedom Approach

In this model, vessels can move in all three horizontal directions. In Hutchison's study a global coordinate system is used (SNAME, 2000).

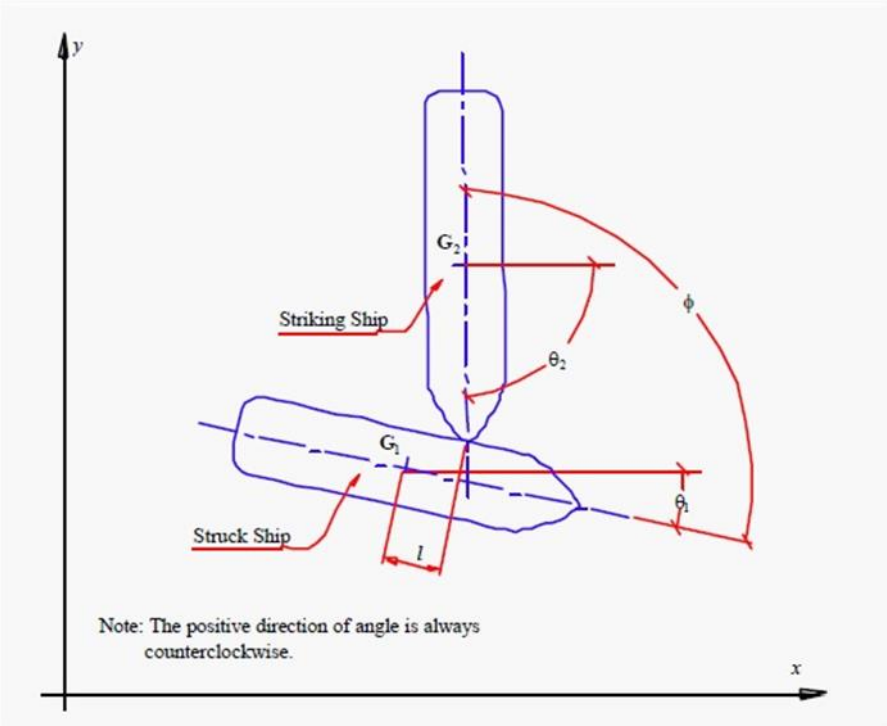

Figure 6 - Global Coordinate System for Both Vessels

The virtual masses of both vessels are taken into account. In that study, some assumptions were made like following;

- Rotations are neglected.
- There is no change in the distrubution of mass after the initial contact.
- After the inelastic collision, both vessels move together (Chen,2000).

Zhang's model also considers three degrees of freedom. In this model, instead of a global coordinate system, three different coordinate points are taken into account as can be seen in Figure 7.

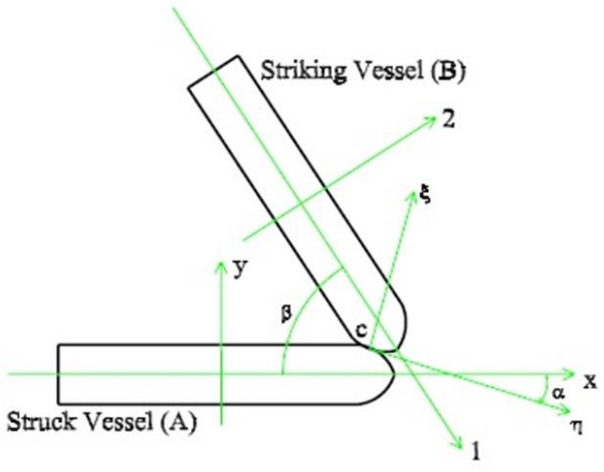

Figure 7 - Origins for Vessels and Striking Point

2.3. Coupled Approach of Internal and External Mechanics Sub-Models

In order to include all above explained effects, a coupled method of both internal and external dynamics is needed. However, as it can be guessed, it would be time consuming to take all the components into account. Thus simplified methods are being used.

By using two dimensional coupled method, Brown used a simplified method (SNAME,2002). Phil and Tabri (2010) have made a finite element simulation with a coupled method, however in the study they neglected buoyancy, gravity and resorting forces while considering the inertia force and the contact force as the most important force components. The buoyancy, restoring and radiation forces are excluded from the model, limiting the motions of the ships to the horizontal plane of the water, the heave, roll and picth motions of the colliding vessels are not considered.

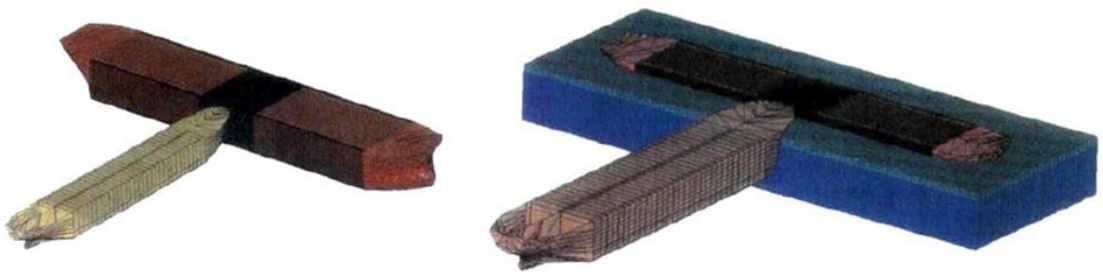

Figure 8 - Combined Model

Le Sourne et al. (2012) presents a user-friendly rapid prediction tool of damage for struck and striking vessels in a ship collision event. To do that, the so-called upper bound theorem is applied to calculate internal forces and energies of any substructure involved in the ships crushing process. At each increment of indentation, the total crushing force is transmitted to the external dynamics MCOL program, which calculates the global ship motion correction by solving the hydrodynamic force equilibrium equations. As a first step, they give a brief description of the upper bound method, originally developed for perpendicular collisions and recently enhanced for oblique ones. Then the theory developed in MCOL program for large rotational ship movements is detailed. By comparing results obtained with and without MCOL, the importance of hydrodynamic effects is highlighted. Some simulation results are compared with results provided by classical nonlinear finite element calculations. Finally, by using the developed analytical tool which mixes internal and external dynamics, different crushing scenarios including oblique collisions are investigated and the influence of some collision parameters like longitudinal and vertical impact location, impact angle, and struck ship velocity is studied (Le Sourne, Besnard, Cheylan, Buannic,2012).

2.4. Experimental Study

Experimental studies are very expensive especially the large-scaled ones. Wevers and Vredeveldt (1999) provided an insight into symmetric collisions with sloshing interactions. The knowledge from the large scale experiments is favourable as it is free of scaling effects however the tests are costly and thus a wide range of collison parameters cannot be studied. On the other hand, model-scale experiments offer an alternative as a wider parametric range can be covered, but special attentio has to be paid to scaling (Tabri, 2010).

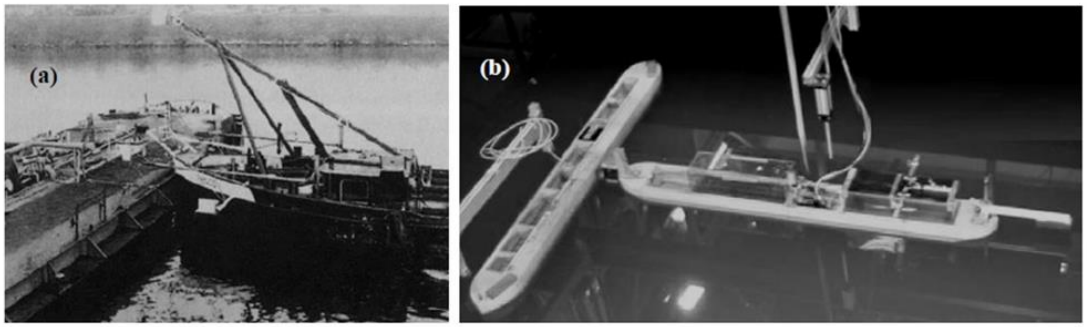

Figure 9 - Model-Scale Experiment

2.5. Finite Element Method

Finite element tool is very useful for ship collision analysis because of the complexity of the problem with the existance of free surface and other fluid effects with structural plastic and elastic deformation. The external dynamics MCOL program was developped and included in LS-DYNA finite element solver by Le Sourne (2003) who used it amongst other to highlight the hydrodynamic effects in ship-submarine and surface ships collisions.

In Figure 10, meshing of the collision analysis can be seen. Only collision areas of both vessels are usually meshed. The rest of the vessels is modeled as a rigid body characterized by its mass center and an inertia matrix. In MCOL, hydrostatic restoring forces, added inertia and wave effects are taken into account.
The example studied is a ship-submarine collision simulation.

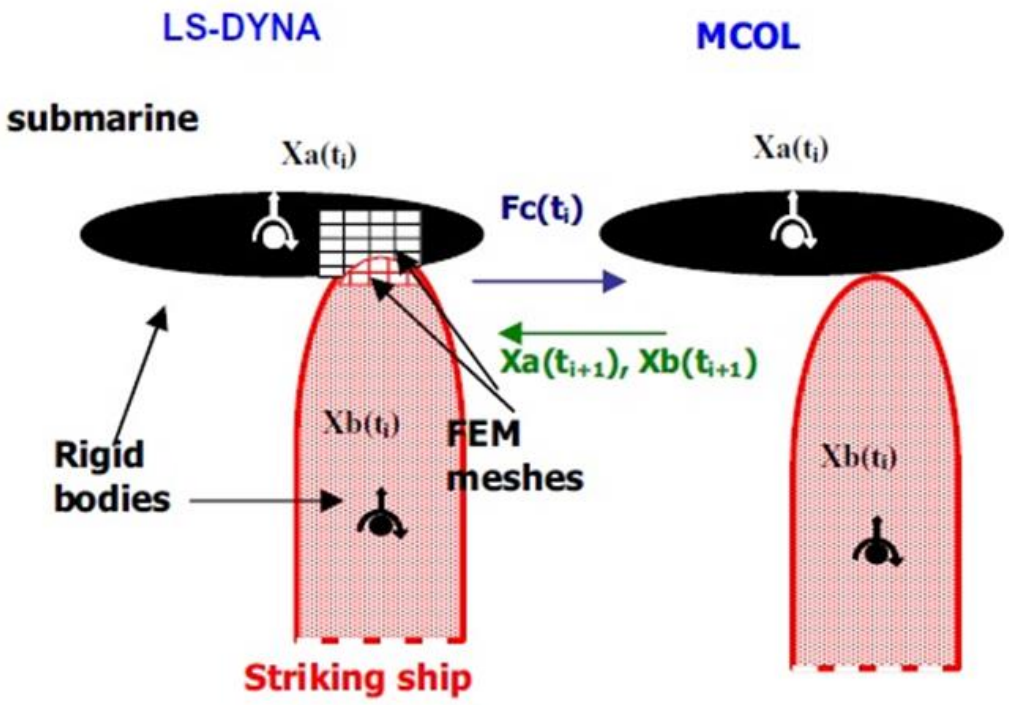

Figure 10 - Ls-Dyna/MCOL Collision Simulation System

Motion equations of ship rigi bodies are solved as follows;

$$[M + M_\infty]\,\ddot{x} + G\,\dot{x} = F_w(x) + F_H(x) + F_v(x) + F_c \qquad (5)$$

Where;

x : The earth-fixed position of the centre of the mass of the ship

M : Structural mass matrix

M_∞ : Added mass matrix

G : Gyroscopic matrix

F_w : Wave damping force vector

F_H : Restoring force vector

F_v : Viscous force vector

F_c : Contact force vector

LS-DYNA can be considered as a reliable tool to study collision cases. But small cell sized mesh is required to obtain realistic results. As can be seen in the following ship to ship collision case, in some conditions LS-DYNA can be used instead of experiment studies.

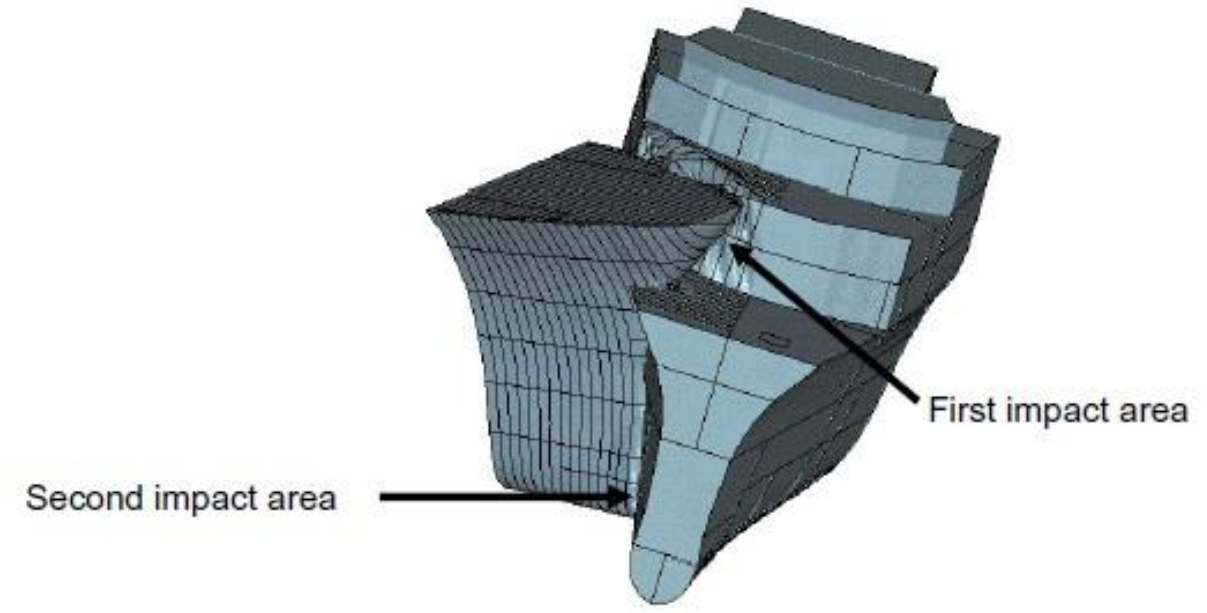

Figure 11 - Ship to Ship Collision Study with Ls-Dyna

In order to see the reliability of the LS-DYNA / MCOL combination, a real accident occured between two military ships was simulated using LS-DYNA/MCOL software. As can be seen in the figures, numerical results match particularly well with photos taken after the accident (Le Sourne et al, 2003).

Figure 12 - Real Ship vs Simulation

Figure 13 - Real Ship vs Simulation from Inside

2.6. Super-Element Method

Although finite element methods usually gives satifaction for ships collision simulation, both meshing and computation is very time consuming. This method is therefore not suited for complete risk collision analyses which may involve several hundreds of scenarios. Moreover, at the pre-design stage, time to conduct a complete finite element analysis is often lacking. In order to show the influence of the structural elements in a short time period, the super-element method may be used. The basic idea of super-element method is to split the vessel into structural macro components which are called super-elements (Paboeuf et al, 2015).

Matematically, during an impact the maximal force F responsible of the collapse of a given super-element with volume V may be obtained by (Buldgen et al, 2012):

$$F\,\dot{\delta} = \iiint_V \sigma_{ij}\,\dot{\varepsilon}_{ij}\,dV \qquad (6)$$

Where;

F : Maximal force responsible for the collapse of a given super-element

$\dot{\delta}$: Penetrating speed of the striking ship in the super-element

V : Component volume to derive the force F analytically

σ_{ij}: Stress tensor of the super-element

$\dot{\varepsilon}_{ij}$: Strain rate tensor of the super-element

In order to solve the equation following hypotheses were made (Buldgen et al, 2012):

- The material of the element is assumed to be perfectly rigid. In other words elastic strains, strain hardening and strain rate effect are neglected.
- The total internal energy rate is obtained by summing the contribution of bending and membrane effects, which are assumed to be completely uncoupled.

The bending and the membrane energy rates can be calculated with the following formulas;

$$\dot{E_b} = M_0 \sum_{k=1}^{m} \dot{\theta_k} l_k \tag{7}$$

$$\dot{E_m} = \frac{2\sigma_0 t_p}{\sqrt{3}} \iint \sqrt{\dot{\varepsilon_{11}^2} + \dot{\varepsilon_{22}^2} + \dot{\varepsilon_{12}^2} + \dot{\varepsilon_{11}}\dot{\varepsilon_{22}}}\, dA \tag{8}$$

Where:

$\dot{E_b}$: Bending energy rate

$\dot{E_m}$: Membrane energy rate

M_0 : Fully plastic bending moment

A : Area of the plate

t_p : Thickness of the plate

$\dot{\theta_k}$: Rotation of the hinge number k

l_k : Length of the hinge number

As explained above, super-elements consist separated macro elements. There are different types of super-elements, an arrangement is explained below as an example (Paboeuf et al, 2015). In order to have a tool which is accurate enough but not too expensive and time consuming Principia and ICAM developed SHARP which is based on super-element method. The tool's speed and accuracy to simulate ship collisions are satisfying in comparison with finite element

analysis (Paboeuf et al, 2015). As in SHARP solver oblique collision are also considered, six type of super-element s have been developed (Buldgen et al., 2012).

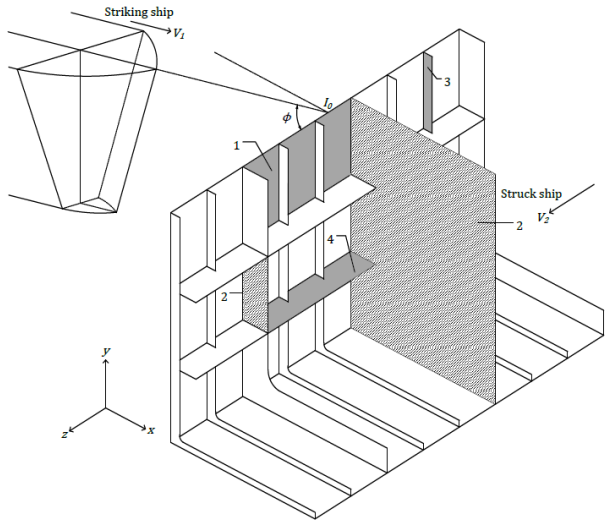

Figure 14 –Different Types of Super-element s

- *Super-element SE1:* a plate simply supported by four edges and submitted to an out-of-plane impact with oblique angle. For example, side shell, inner side shell, longitudinal bulkhead.
- *Super-element SE2*: a vertical plate simply supported on three edges with the remaining free edge. Collision is occurred on the free edge at an angle other than 90 degree. For example, transverse bulkhead.
- *Super-element SE3:* this element is similar to SE2 except collision is occurred inside the structure and the modes of deformation are different. For example, transverse bulkhead, web girders, frames, etc.
- *Super-element SE4:* beam element which is considered to be clamped at both ends. For example, longitudinal stiffeners.
- *Super-element SE5:* this element is absolutely similar to the X-T-L form intersections already mentioned above. The only difference is that the collision angle is assumed to be different from 90 degree. For example, junction of vertical and horizontal structural members.
- *Super-element SE6:* a horizontal plate, simply supported on three edges and free on the last one. Structure is similar to vertical one considered in SE2 and SE3. Collision is assumed to occur at the unsupported edge with a certain angle in the horizontal plane (See Figure 10f). For example, weather deck.

2.7. SHARP Tool

SHARP is an effective ship collision analysis tool which is based on super-element method. In 2006, MCOL program was adapted to be used in SHARP as well. In other words, external dynamics are included in SHARP and both ship can also be assumed to move and rotate in three degrees of freedom.

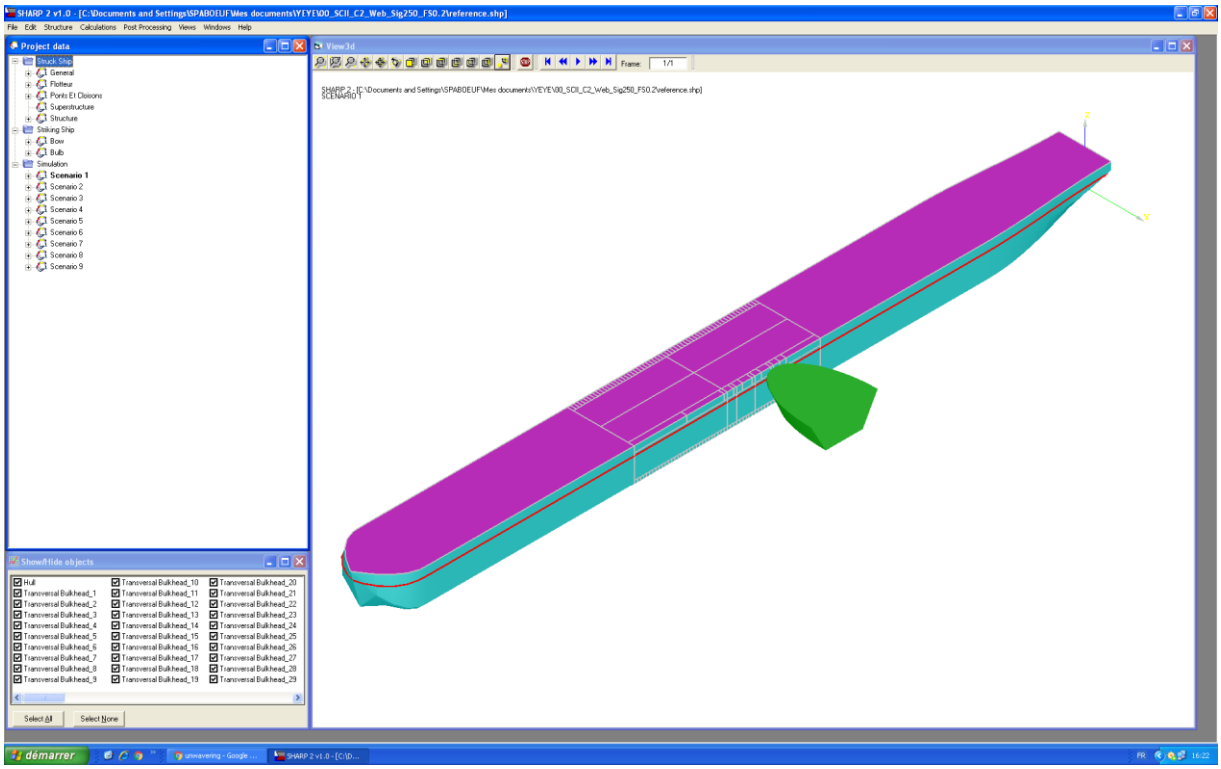

Figure 15 – Graphical User Interface of SHARP (Sone Oo, 2017)

In Figure 15, graphical user interface of SHARP can be seen. Also simulation can be viewed visually including external dynamics and structural responses such as failure or activation of a structural super-element.

In SHARP, striking ship's deck is defined with an ellipse equation and bow-side angles are also required to define model. In order to save time during the modeling phase, struck ship scantling is defined just around the collision area (the described area is often bounded by two transverse bulkheads). Once both vessels are modelled, collision point and angle should be indicated. Thanks to ability of defining different collision scenarios, that arrangement can be used to calculate several collisions only by specifying desired collision points.

Flowchart of SHARP software can be seen in the following figure (Le Sourne et al.,2012).

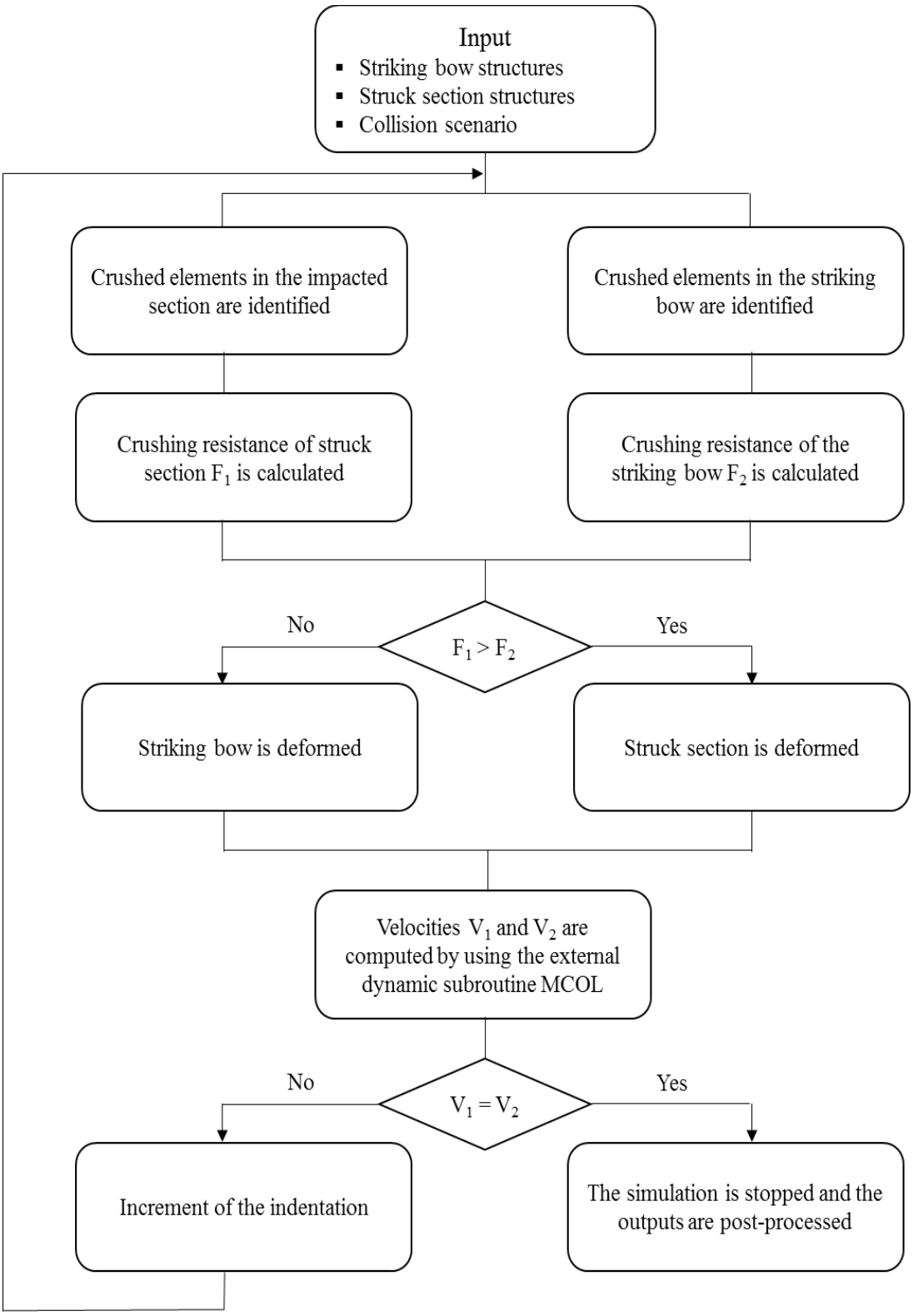

Figure 16 – Workflow of SHARP (Le Sourne et al.,2012)

Thanks to MCOL, external ships dynamics is considered during the collision simulation. SHARP without MCOL can only be used to simulate collisions against ships which are moored to a quay and, as a consequence, not supposed to move.

Post processing of the result can be made in SHARP's graphical user interface as well. Internal energies, resistance forces and ship motions can be analyzed.

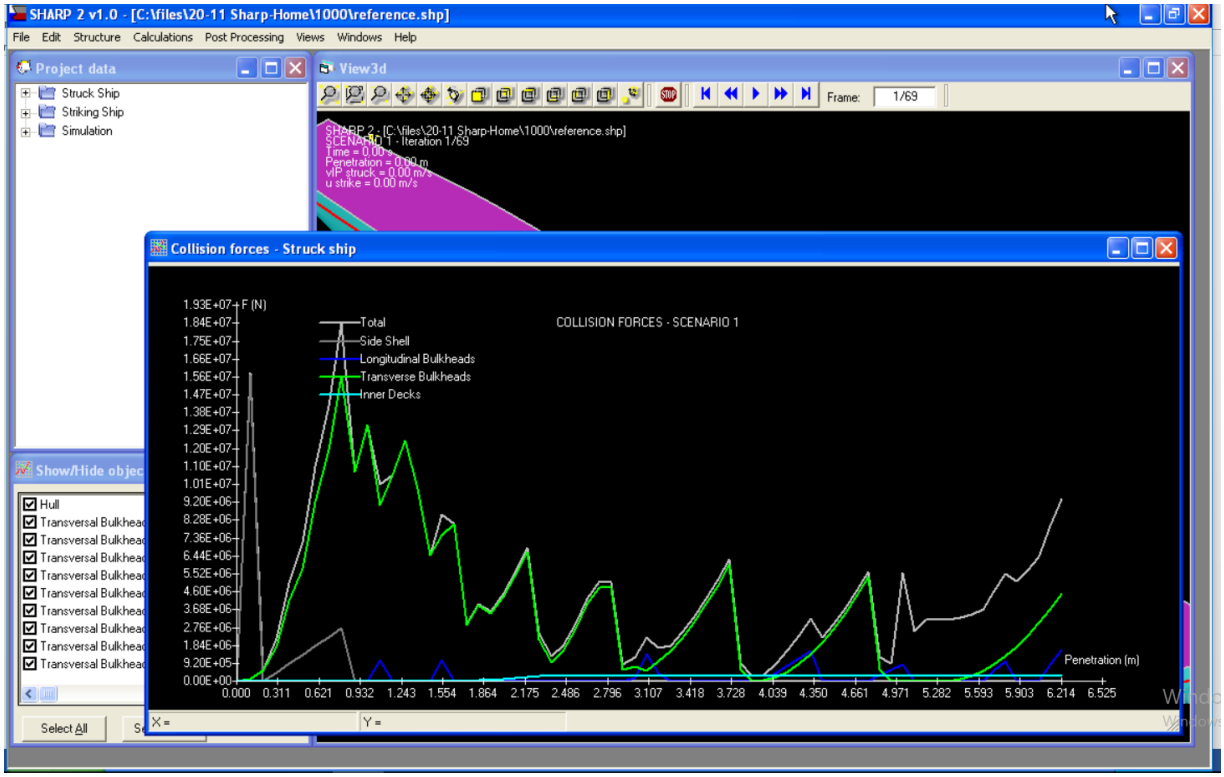

Figure 17 – Example for SHARP's Post Processing Module

It is worth noting that all above numerical results are also written in text files. Thanks to this feature, calculations related to the present master thesis were made easily.

3. RESULTS AND CONCLUSION OF PREVIOUS STUDY

In the thesis studied by Sone Oo (2017), SHARP software was tested for different scenarios. Same collision scenarios were simulated both in SHARP and Ls-Dyna and results were compared. In present work, some of these scenarios will be simulated again in order to implement additional functionalities. In previous master thesis, both striking V-shape and barge bows were tested. However; it was stated that as long as drawing interface of SHARP is not advanced enough, barge bow could not be modelled precisely. In following figure, inefficiency of drawing interface is explained by Sone Oo (2017).

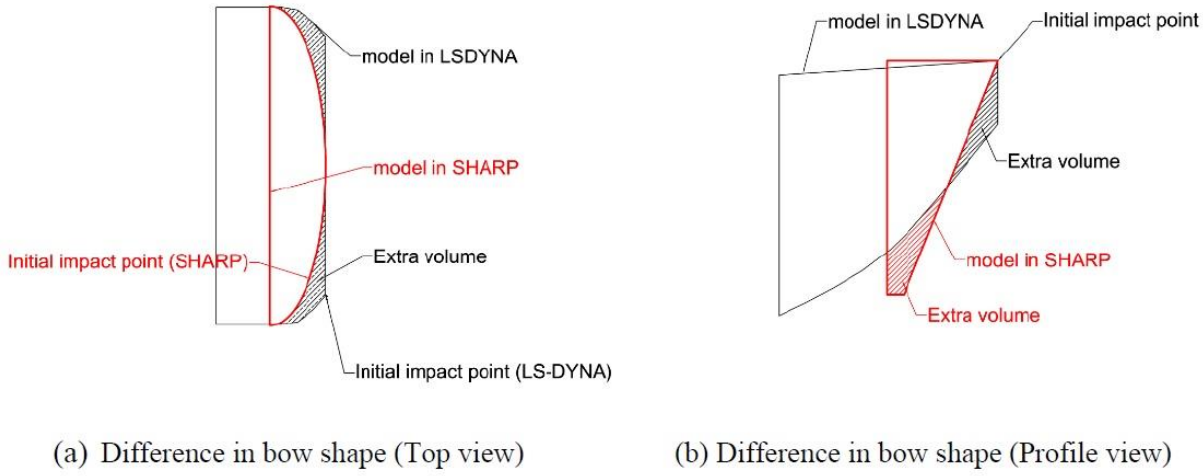

Figure 18 - Barge Bow Modelling in both SHARP and Ls-Dyna

Therefore; in the present work, collision scenarios which simulated with barge bow will not be studied again. Besides, because this paper is focused on collisions in scope of ADN Regulations, oblique collision scenarios with V-shape bow will be excluded as well. In present work, collision scenarios where a V-shape bow is impacting at different depths the struck ship with 10 m/s of velocity will be simulated and results will be presented.

3.1. Case-1 - Collision Point is Just Below the Deck of Struck Ship

In this case, collision point is just below the weather deck of struck ship. Perspective view can be seen in Figure 19. This collision case can represent a case when the depths of both striking and struck ships are close to each other which is a general situation for inland navigation vessels.

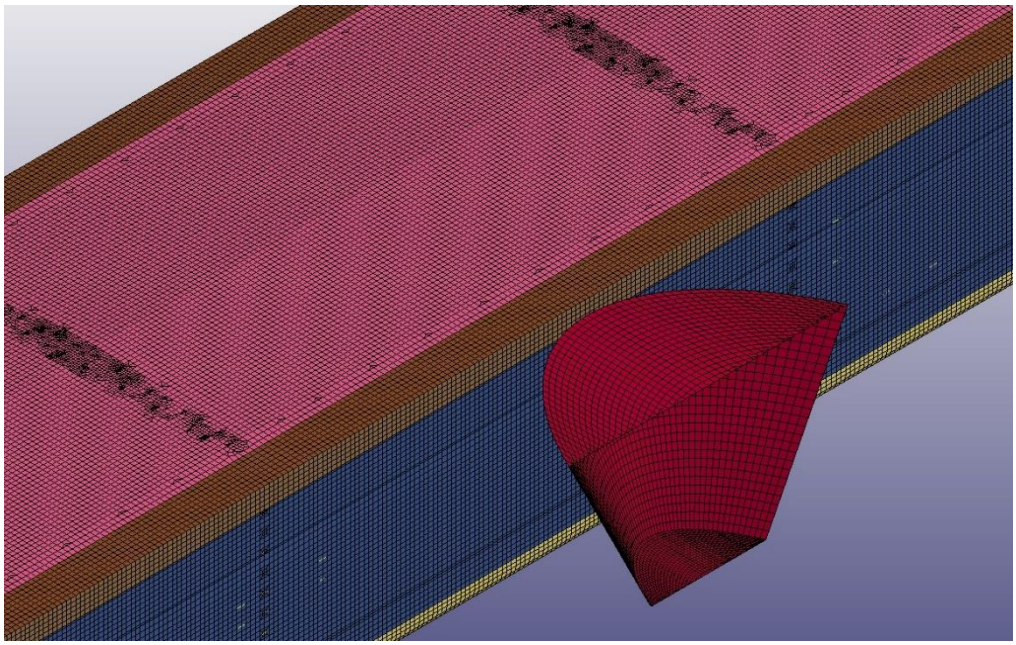

Figure 19 – Perspective View of Collision Point for Case – 1

Front view of the collision point can be seen in the following figure. Same scenario is also simulated in SHARP.

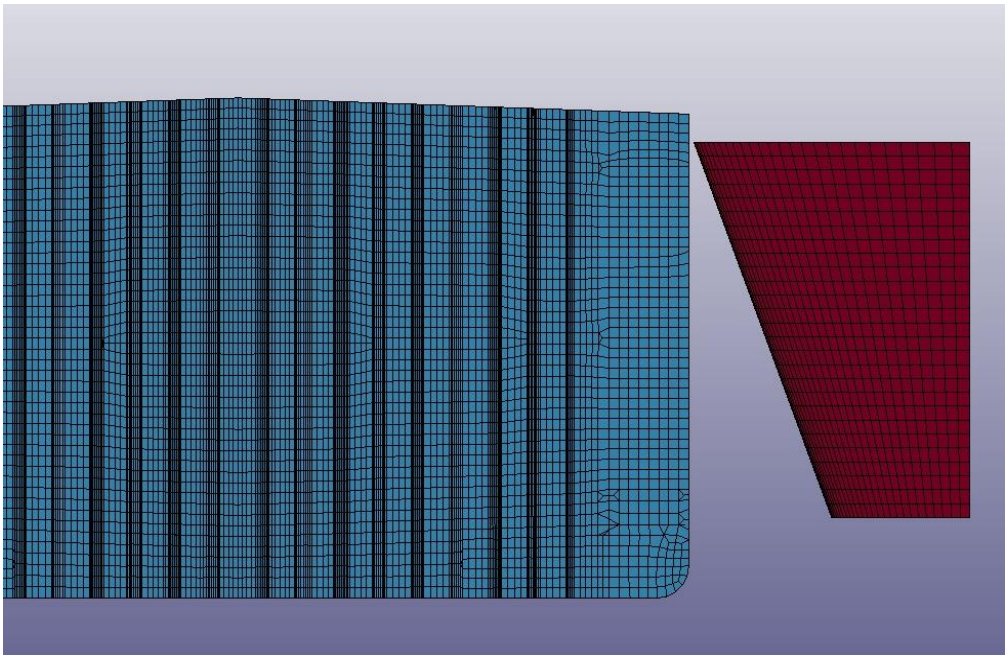

Figure 20 - Front View of Collision Point for Case – 1

Nonetheless, in SHARP software, super-elements are activated after the contact between the striking ship and regarding element has occured. Because of that; in SHARP, each case is simulated with 9 different collision points.

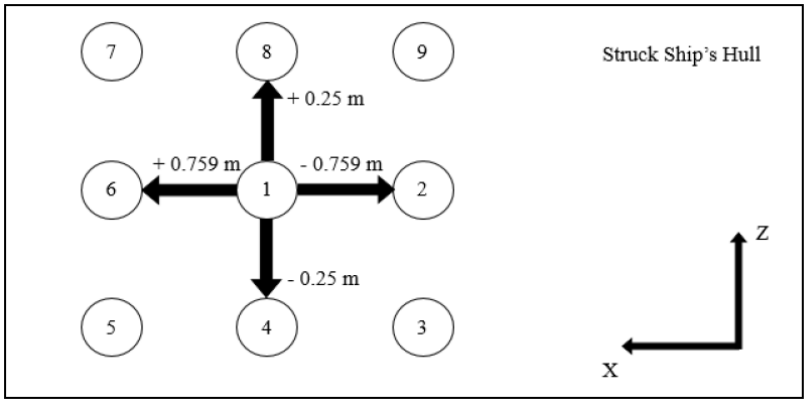

Figure 21 - 9 Collision Scenarios for SHARP

Space between different collision points in X direction is half length of the distance between web frames. Likewise in Z direction, spacing is half distance of stiffner spacing. The main goal of this arrangement is to activate different super-elements in vicinity of the collision area. After all the scenarios will be run, the average of all nine points will be assumed as final result.
It should also be noted that because of ADN regulations, all the results will be evaluated until 1 m of penetration which is the maximum distance between the side shell and longitudinal bulkhead. The comparison of the results for collision Case – 1 can be seen in the table below.

Table 1 - Results of Collision Case – 1

1000-Case	**Deformation Energy [MJ]**
LS-DYNA	5.79
SHARP (Average)	5.03
% Difference	13%

The discrepancy between super-element tool and finite element software is around 13% and SHARP is conservative for this case.

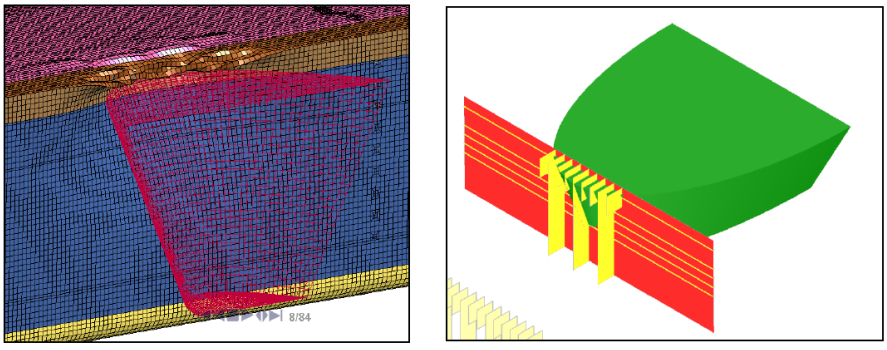

(a) LS-DYNA (b) SHARP

Figure 22 - Models in Ls- Dyna and SHARP after 1 m of Penetration

As concluded in previous thesis by Sone Oo (2017), the discrepancy comes from the lack of post rupture resistance of the side shell which is modelled by super-element – 1 and also by the lack of coupling between side sheel and weather deck.

Yellow color in SHARP's visual interface represents activated elements, while red color distinguishes failed elements. As it can be seen in Figure 22, side shell in Ls-Dyna is unperforated, on the other hand it is failed in SHARP. Thus side shell is not contributing to total internal energy after rupture moment. Likewise in Ls-Dyna, deck is deforming with side shell while it is not activated in SHARP, hence there is not any contribution to total internal energy by weather deck neither.

3.2. Case - 2 - Collision Point is Around Mid – Depth of Struck Ship

In second case which will be examined in present thesis, collision point is around mid – depth of the struck ship. This collision case can represent the collision when striking ship's freeboard is much smaller than the freeboard of struck ship.

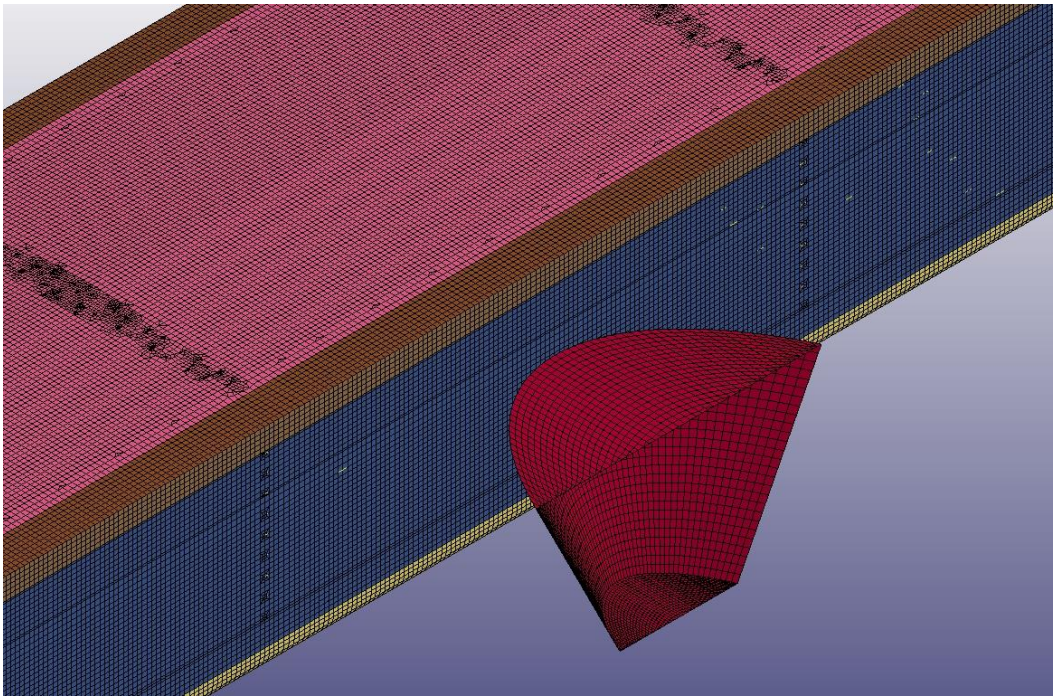

Figure 23 - Perspective View of Collision Case – 2

This case can also be expressed as the one which coupling effect between side shell – weather deck and side shell – bottom plate is the lowest. Because the collision point is far from the boundries.

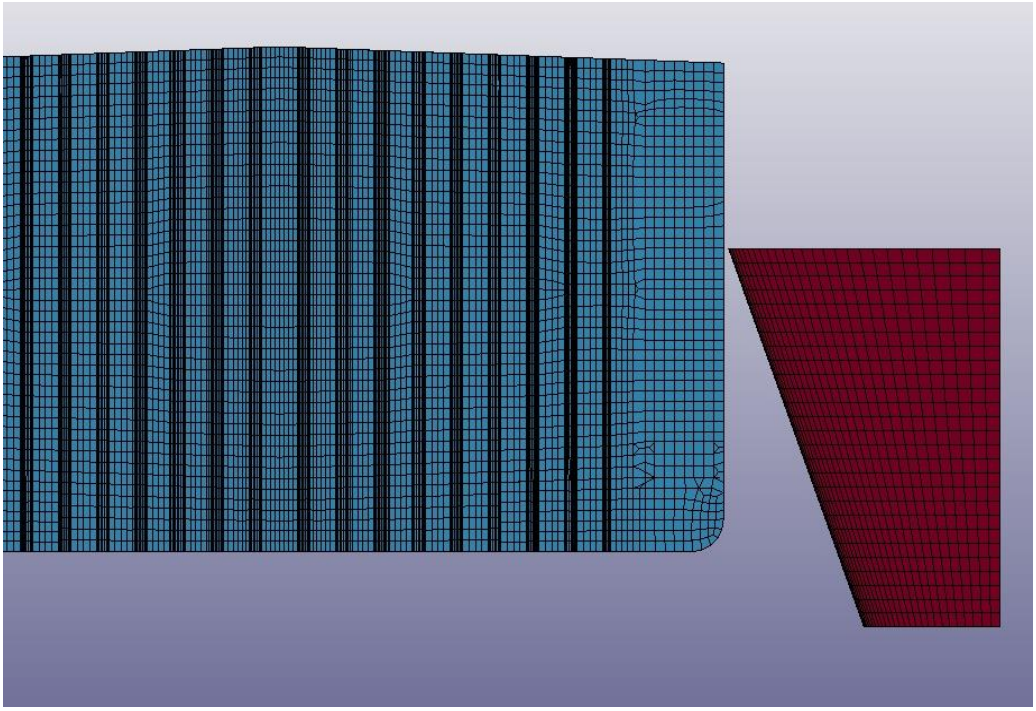

Figure 24 - Front View of Collision Case – 2

Same orientation for 9 different collision scenarios in SHARP has been applied for this case as well. And the comparison of the results can be seen in the table below.

Table 2 - Results of Collision Case – 2

2000-Case	**Deformation Energy [MJ]**
LS-DYNA	4.49
SHARP (Average)	1.05
% Difference	77%

In this case, the discerepancy between final internal energy at 1 m penetration in Ls – Dyna and SHARP is around 77% which is not acceptable. Main difference in this case is because of lack of post rupture resistance. The side shell fails in the beginning of the simulation and resistance force for that element directly goes to zero. As a result until 1 m of penetration, there is no contribution to total internal energy by the side shell after rupture moment.

Besides even the collision point far from the deck and bottom boundries, the coupling effect between the web frames has a notable outcome as well. In SHARP only the elements which are physically contacted with the striking ship are activated. On the other hand in Ls – Dyna all the elements which are in vicinity of the collision point absorb energy. Thus total energy is higher in Ls - Dyna than SHARP.

3.3. Case – 3 – Collision Point is Just Above the Deck of Struck Ship

In present case collision point is above the weather deck of struck ship, thereupon it can be said that deck super-element will be activated in SHARP during this simulation.

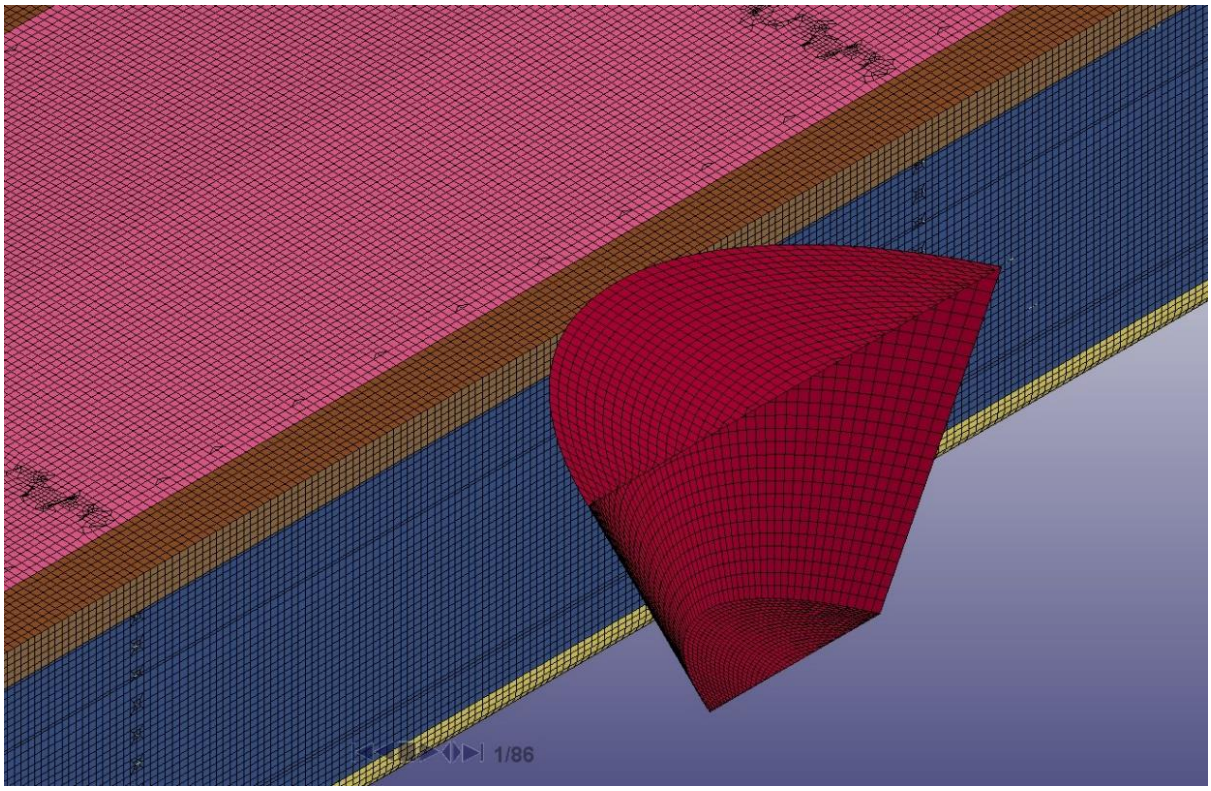

Figure 25 - Perspective View of Collision Case – 3

Because weather deck super-element is in collision area, coupling effect between deck and side shell is expected to be relatively less in this case. In order to make a guess about the effect of post-rupture resistance of side shell, it is necessary to know the rupture moment. As it can easily be understood; if rupture occurs after 1 m of penetration, post rupture resistance will be neglected in present work.

For this particular case, it should also be remarked that final penetration calculation is slightly different than other cases. Because the tip point of the striking ship is not in contact with the struck ship, final penetration of the striking ship will vary according to the height of the striking point. In other words; with same surge of striking ship, total penetration will be less in SHARP.

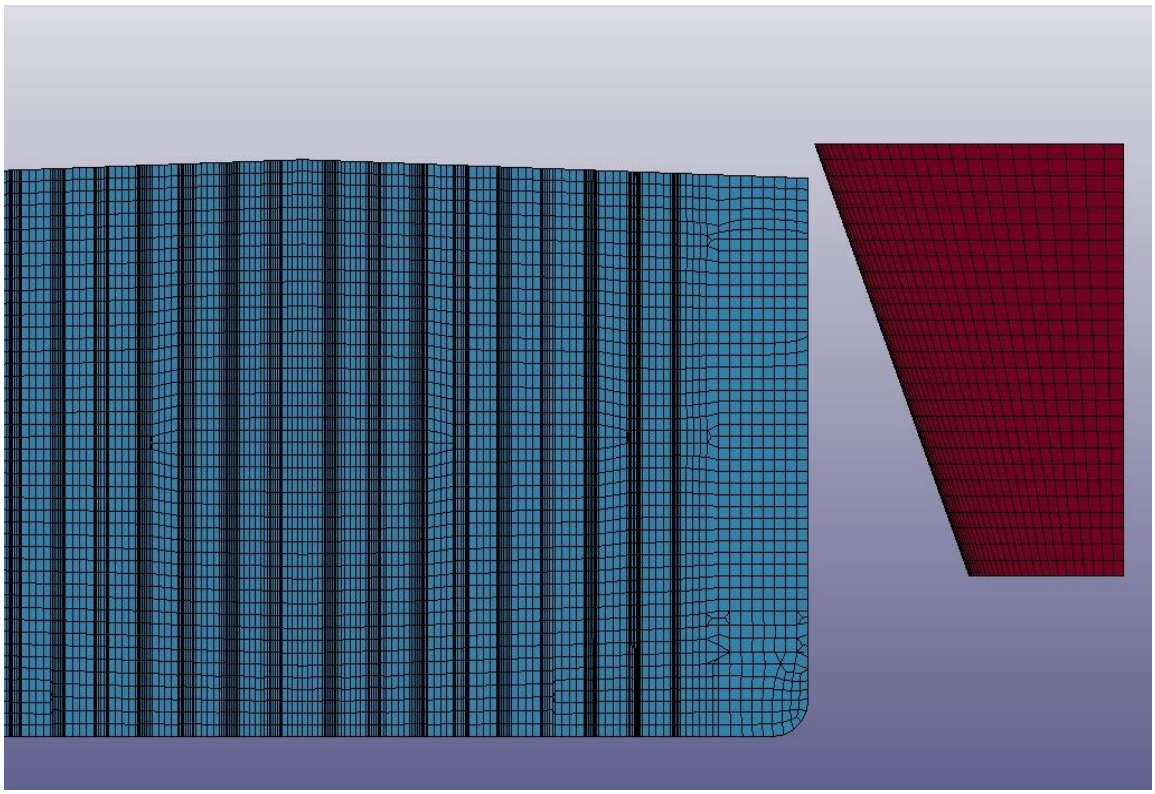

Figure 26 - Front View of Collision Case - 3

The comparison of the results which obtained from both Ls-Dyna and SHARP simulations can be seen in the table below. Also it is necessary to point that rupture moment is reached after 1 m of penetration. All in all it is expected that effects of both coupling between side shell-weather deck and lack of post rupture resistance will be relative less important in this scenario.

Table 3 – Results of Collision Case - 3

5000-Case	**Deformation Energy [MJ]**
LS-DYNA	6.68
SHARP (Average)	7.21
% Difference	-8%

For the last case, the discrepancy between finite elements tool and super-elements software is relatively less (around 8%) and results given by SHARP are considered to be acceptable. Furthermore, in consideration with the time required for preparing the models and for computation, SHARP can be commented as an effective tool because total required time is only minutes for SHARP while it will take several days with Ls-Dyna.

4. POST RUPTURE RESISTANCE IN SHARP

4.1. Lack of Post Rupture Resistance

As it is explained above; in SHARP solver, resistance of all super-elements is directly forced to zero when rupture occurs. As a result, after first failure moment, side shell which is represented by super-element -1 is not absorbing anymore energy in contrary with reality.

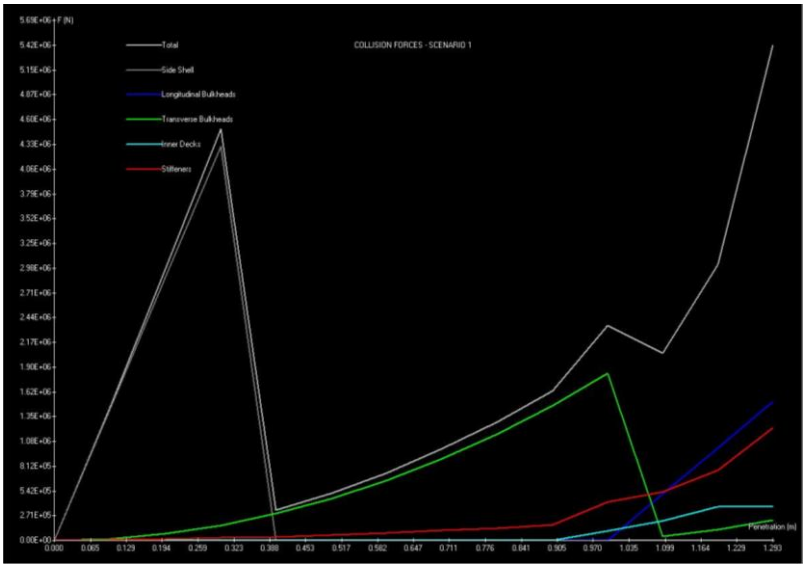

Figure 27 - Example of Resistance for After Rupture

Even it seems like the resistance force is decreasing linearly in the figure above, it is only because of the continuity between successive time steps. Likewise it can be seen in the figure below that the side shell does not contribute anymore to total the energy once rupture has occurred.

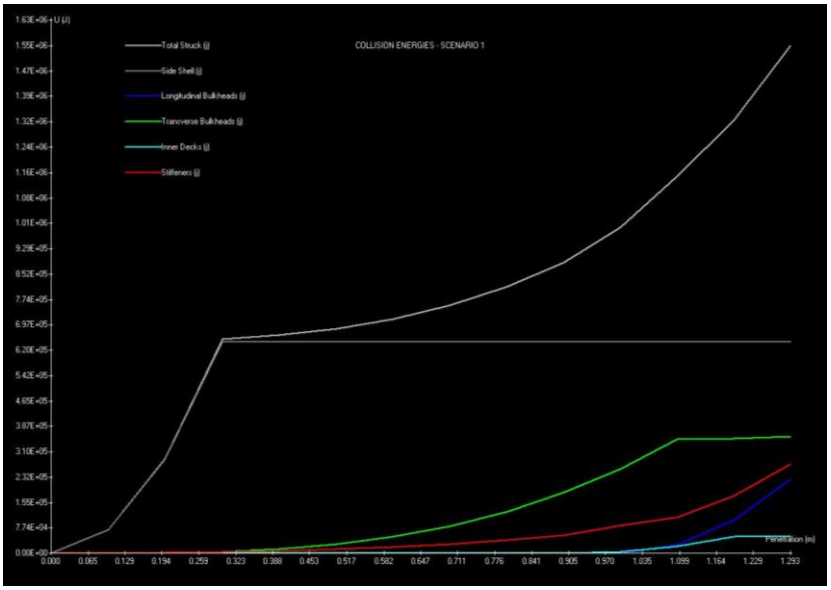

Figure 28 - Example of Total Internal Energy After Rupture

4.2. Hypothesis to Calculate Post Rupture Resistance

In order to calculate the resistance force of a ruptured super-element, a hypothesis has been suggested in present study. It is assumed that when ruptured area becomes equal to the sectional area of the striking ship, then corresponding super-element does not resist anymore. So in other words according to this hypothesis, resistance force of a ruptured shell element is decreasing proportionally to striking ship's sectional area at corresponding time step.

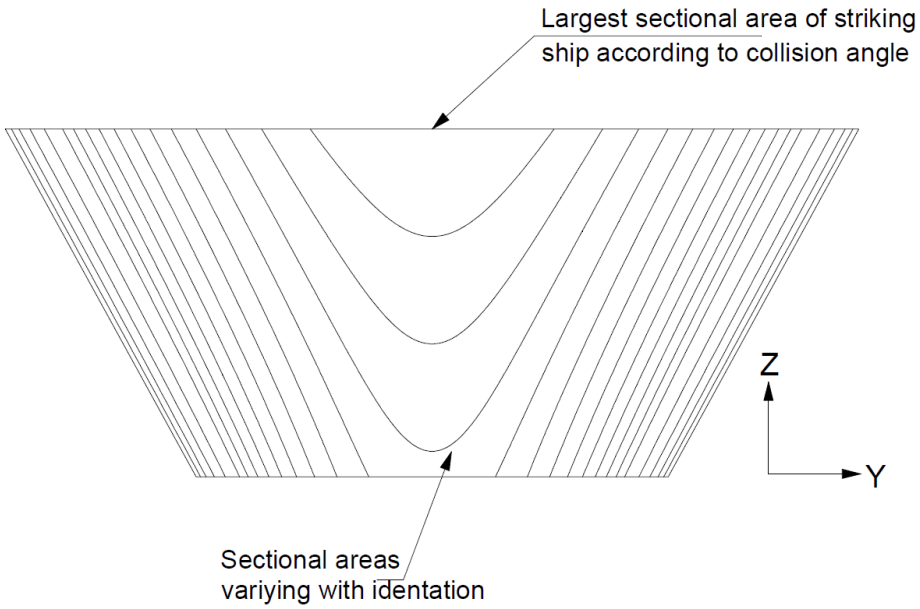

Figure 29 - Sectional Areas of Striking Ship

Therefore the resistance force of a ruptured shell element (which is super-element 1 according to SHARP) for a particular penetration value can be calculated with the formula below.

$$F = Fmax - (Fmax * \frac{Area\ @\ Corresponding\ \delta}{Largest\ Area}) \quad (9)$$

In this study, the ruptured area of the struck ship, which is assumed to be equal to the striking ship's sectional area at corresponding penetration value, will be called *non-resisting area*. Likewise the difference between the sectional area of the striking ship at final penetration value and non-resisting area will be called *resisting area*. Thus the hypothesis can be explained as; the ratio between the resisting area and maximum sectional area will be equal to the ratio between the resistance force of same element at corresponding penetration and the maximum resistance force (which is just before the collapse moment).

4.3. Determining Non-Resisting Area

As it is explained above, non-resisting area is assumed to be equal to the sectional area of the striking ship at corresponding time step and penetration value. But elastic deforming of side shell element is also needed to be taken into account.

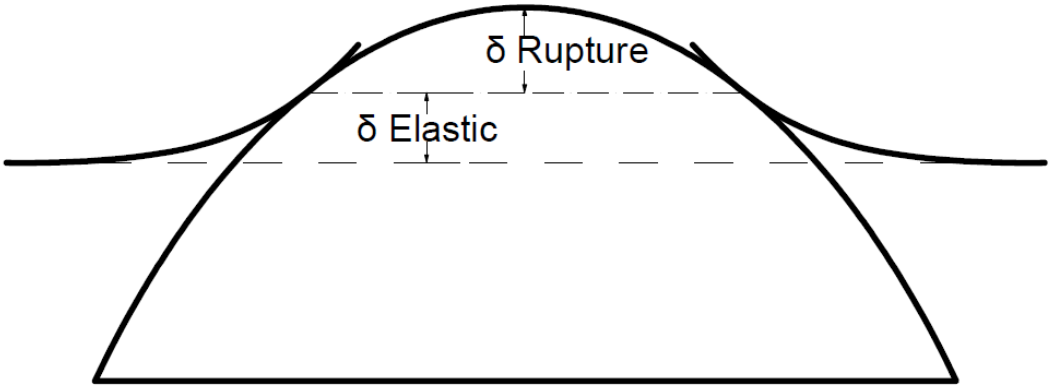

Figure 30 – Determining Penetration

It is assumed that ruptured area of the shell element will be equal to the sectional area of striking ship at corresponding penetration. But it should also be noted that shell element will deform elastically before failing. In the present work, the difference between the total penetration and elastic penetration will be called 'Rupture Penetration ($\delta_{Rupture}$)'. Following figure which is taken from Ls-Dyna simulation demonstrates this difference.

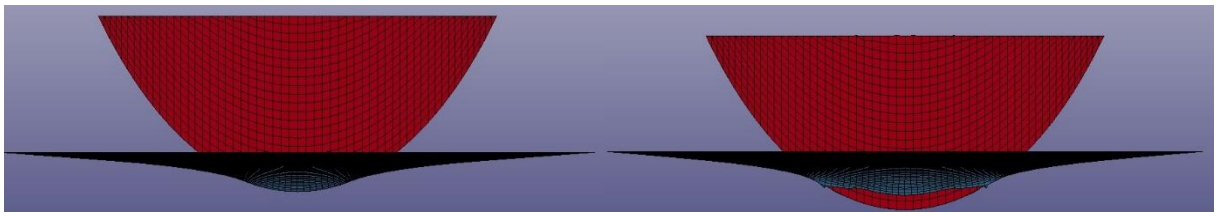

Figure 31 - Total Penetration and Rupture Penetration

In the figure above, successive time steps of a basic simulation is shown. The figure on left side shows the time step which is just before the rupture moment and on right side the rupture moment is shown. This figure indicates that it is better to use $\delta_{Rupture}$ instead of δ_{Total} in order to calculate non-resisting area. But in order to see the results for different collision scenarios, post rupture resistance will be calculated from both total penetration and rupture penetration. The results of both situations will be presented.

4.4. Basic Trials with New Hypothesis

The method was tested with a basic scenario in order to see if the results are consistent with Ls-Dyna ones. A rectangular shell element which height is 9 m and width 12 m was clamped on four edges. As striking ship, the model of Sone Oo (2017) was chosen and striking velocity was 5 m/s. Besides, 3 different collision points were chosen in order to evaluate the importance of the distance between the collision point and boundaries. The arrangement can be seen in the figure below.

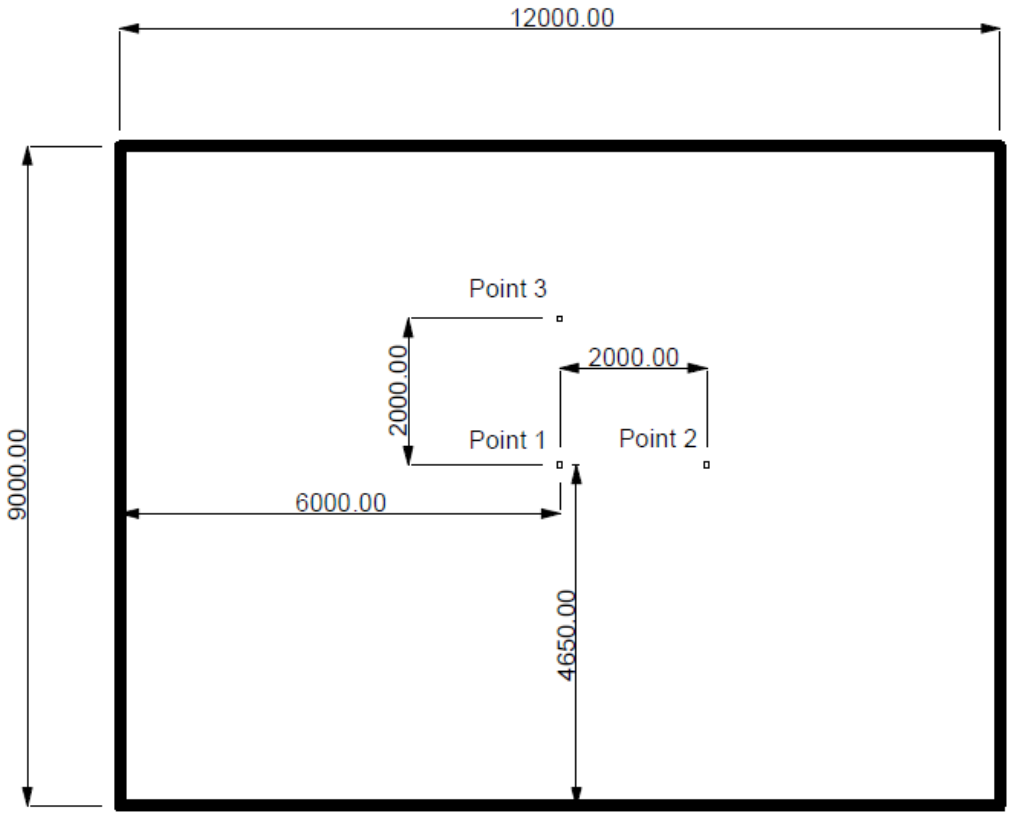

Figure 32 - Arragement of Collision Points for Basic Case

The first collision point was positioned 4.65 m away from the bottom edge, because the height of the striking ship was equal to that value. The main goal was not to be in contact with bottom boundary. For the same reason, second collision point has been chosen 4 m away from the right edge, because the width of striking ship was 8 m. Third point was 2.35 m away from the top edge.

The striking ship was set as rigid body and rectangular panel is assumed to be made with steel. Failure strain is set to 0.2 which is same value as the one used in previous study by Sone Oo (2017). The thickness of the panel is varied for different trials.

Sectional areas of the striking ship were calculated by another 3D modelling software in order to be accurate. But it should be noted here that, in SHARP solver, the sectional areas have to be calculated analytically.

4.4.1. Basic Trial for Point – 1

For the trial with Point - 1 which is in the center, panel thickness was set to 50 mm and simulation period was 1.5 seconds. Because a relatively thick panel was used, striking ship did not pass through the clamped panel.

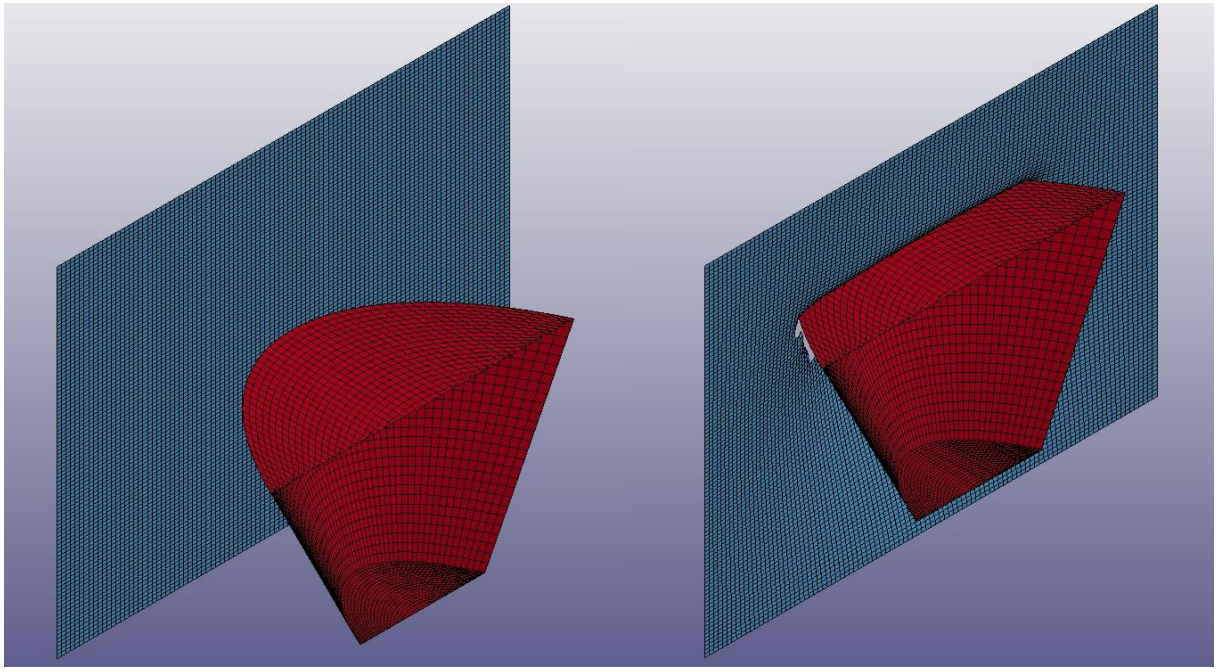

Figure 33 - First and Final Time Steps for Point – 1

In order to calculate the post rupture resistance of the perforated panel with above mentioned hypothesis, final indentation and sectional areas of the striking ship have to be known. Final indentation was taken from Ls-Dyna simulation for basic trials. But it should also be noted here that in SHARP, that value is not known during the simulation. So that the hypothesis has to be improved in order to be used in SHARP. This improvement will be explained in the following sections. Concerning sectional areas of the striking ship, same model was drawn in a 3D modelling software. In previous study by Sone Oo (2017), model was drawn in SHARP. Thus the deck and bottom edges of the V-shaped bow are ellipses. Besides the stem and side angles are known. By using these values, a model was created and sectional areas at related

penetrations were calculated accurately. In this section, Formula 9 was used to calculate post rupture resistance. Maximum resistance force and penetration values were taken from Ls-Dyna and areas were calculated by a 3D modelling software. The comparison between calculated post rupture resistance and the one taken from Ls-Dyna simulation can be seen in the figure below.

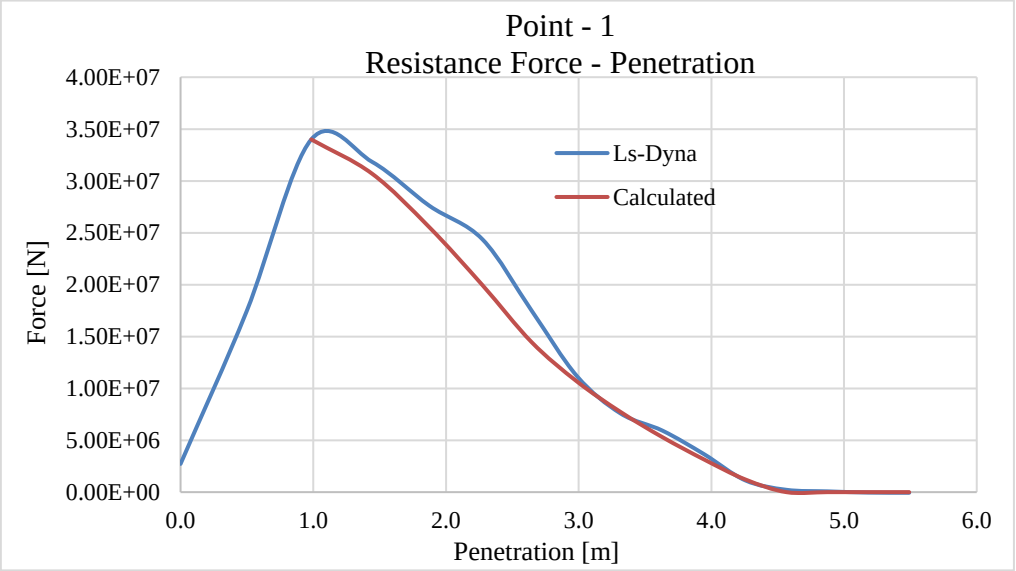

Figure 34 - Comparison of Resistance Forces for Point – 1

Calculated post rupture resistance forces were in a good consistence with the ones post-processed from finite element simulations. And by integrating resistance forces, total internal energy absorbed by the clamped panel after rupture was calculated. Comparisons of the results can be seen in following figure.

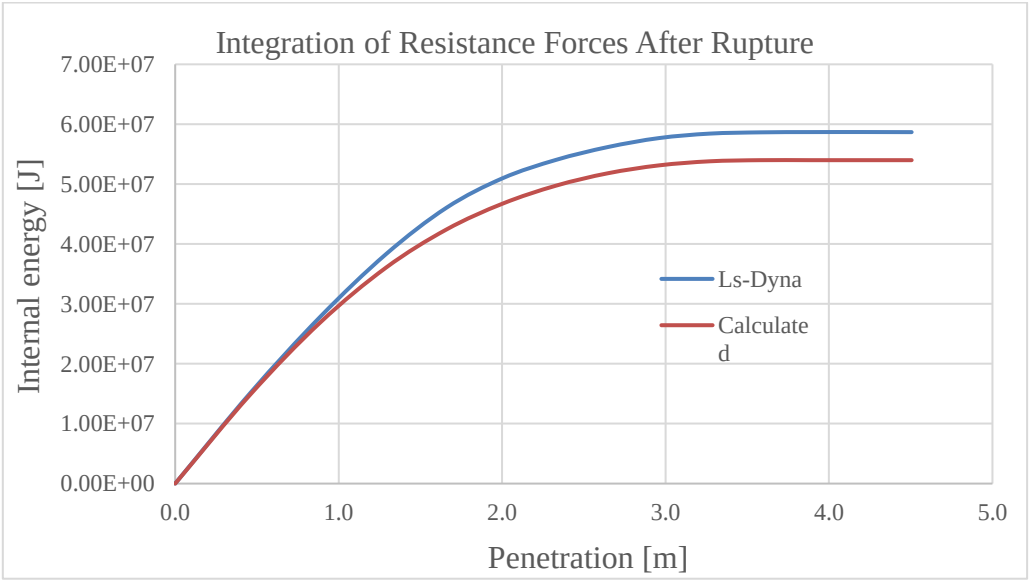

Figure 35 - Comparison of Internal Energies for Point – 1

As it can be seen in the figure, calculated post rupture energy is close to numerical one and is conservative. The discrepancy can be seen in the following table.

Table 4 - Discrepancy in Internal Energies for Point - 1

Absorbed Energy After Rupture (in Joules)			
By	LS-Dyna	Calculated	Discrepency
Point-1	5.88E+07	5.40E+07	8.23%

The discrepancy between analytical and numerical energies is around 8% for Point – 1 which can be commented as acceptable.

4.4.2. Basic Trial for Point – 2

The basic trial for Point – 2 was run with same material properties. But in order to show that the thickness of the basic panel does not have any influence on results, outcomes of the trial which was done with a relatively thinner plate will be presented in this section. The thickness of the steel panel was set to 10 mm for Point – 2.

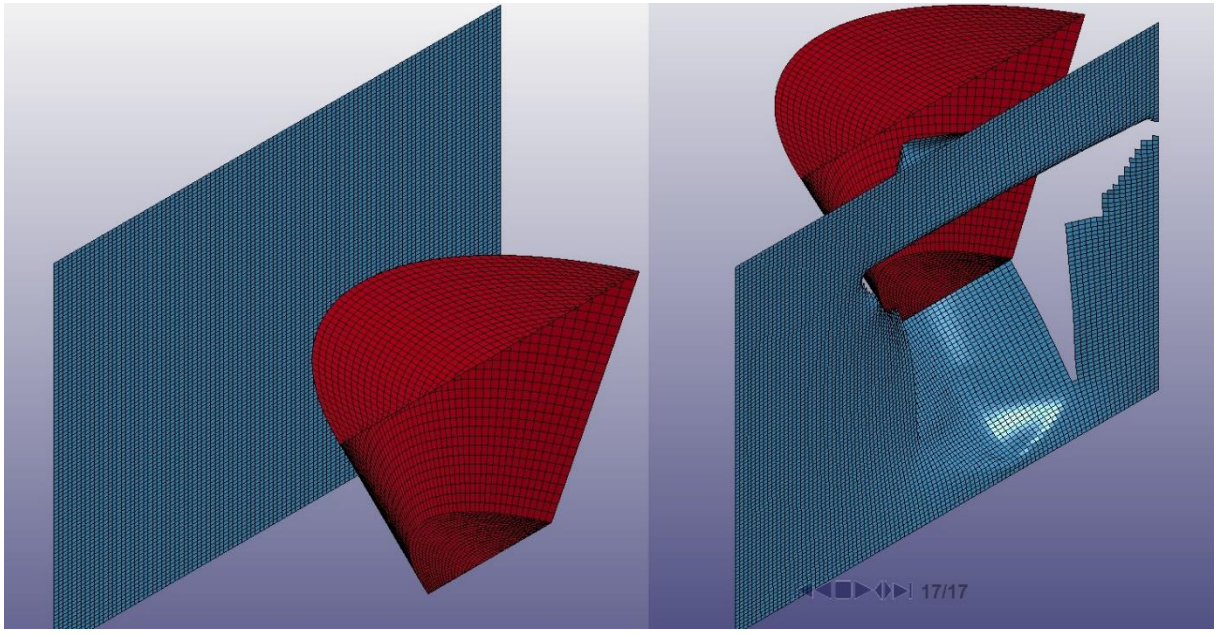

Figure 36 - First and Final Time Steps for Point – 2

As the plate thickness was lower than the one for Point – 1, the striking ship passed through the basic panel. Also it should be noted that striking ship's right edge touched the boundary of the panel which was chosen as a limit for basic trials.

The comparison of the post rupture resistance forces can be seen in the following figure.

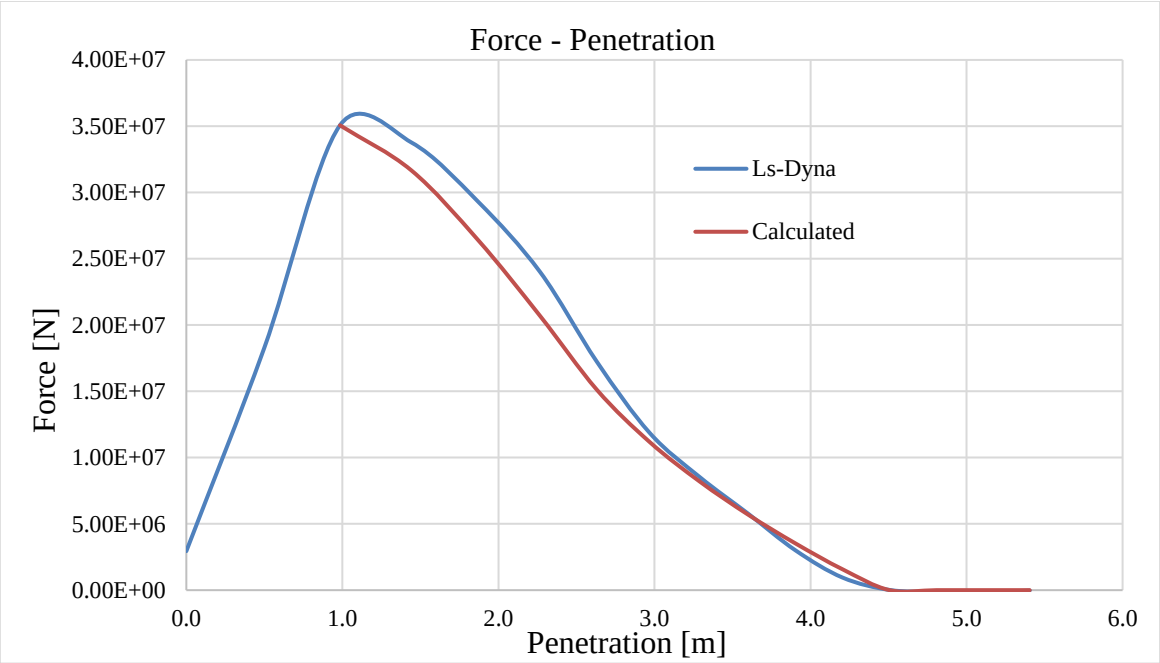

Figure 37 - Comparison of Post Rupture Resistances for Point - 2

Likewise, calculated post rupture resistance of collision point-2 is in good correlation with FE results. Comparison of the internal energies absorbed by panels can be seen in the following figure.

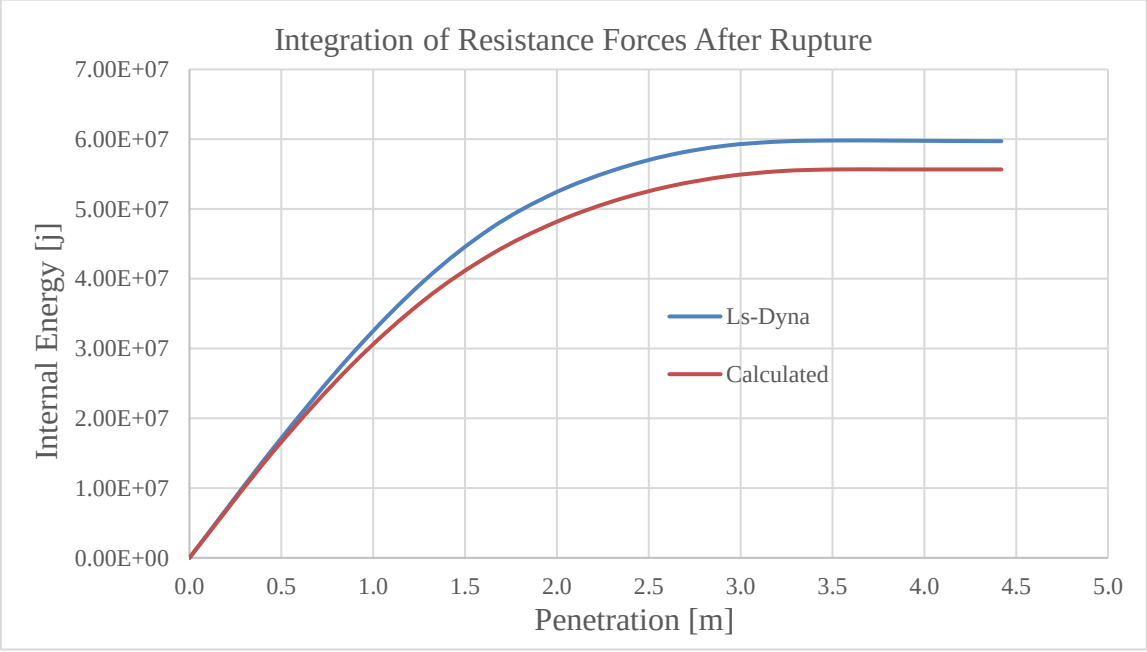

Figure 38 – Comparison of Internal Energies for Point -2

Calculated absorbed energy by integration of the post rupture resistance forces shows a reliable consistency with the one which post-processed from Ls-Dyna. The discrepancy can be seen in the table below.

Table 5 – Discrepancy in Internal Energies for Point - 2

Absorbed Energy After Rupture (in Joules)			
By	LS-Dyna	Calculation	Discrepency
Point-1	5.98E+07	5.57E+07	6.91%

The discrepancy is about 7%. That value was around 8% for Point – 1. Even the thickness and the distance from the boundary were different for two cases, it can be said that both discrepancies are close to each other and they can be commented as acceptable.

4.4.3. Basic Trial for Point – 3

For point 3 material properties were kept same but the thickness of the plate was set to 20 mm. Velocity of the striking ship was also 5 m/s and termination time of the simulation was 1.5 seconds. Visuals of the first and last moments can be seen in the following figure.

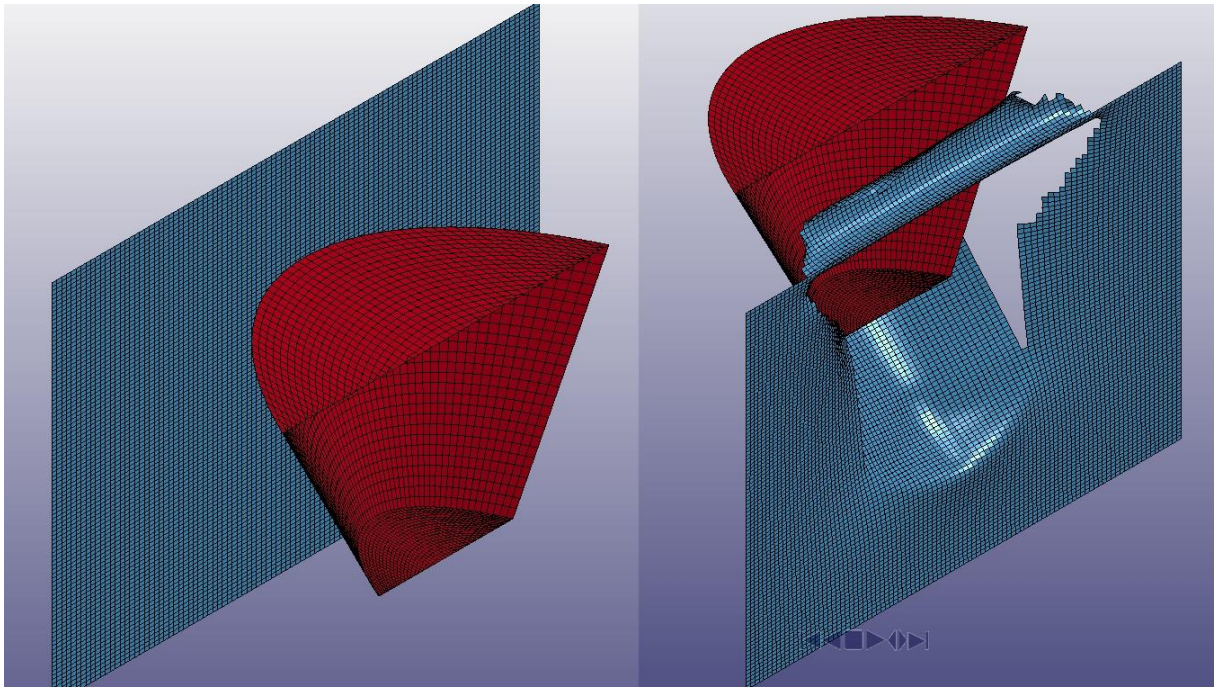

Figure 39 – First and Last Time Steps for Point – 3

Also in this simulation, striking ship passed through the clamped panel. It should be noted here that for Point – 2 and Point – 3; while calculating the largest area of the struck ship, maximum

sectional area was used. But for Point – 1, largest area is equal to the sectional area at final penetration which is smaller than the maximum sectional area of V-shaped bow.
Comparison of the post rupture resistance forces for Point – 3 can be seen in the figure below.

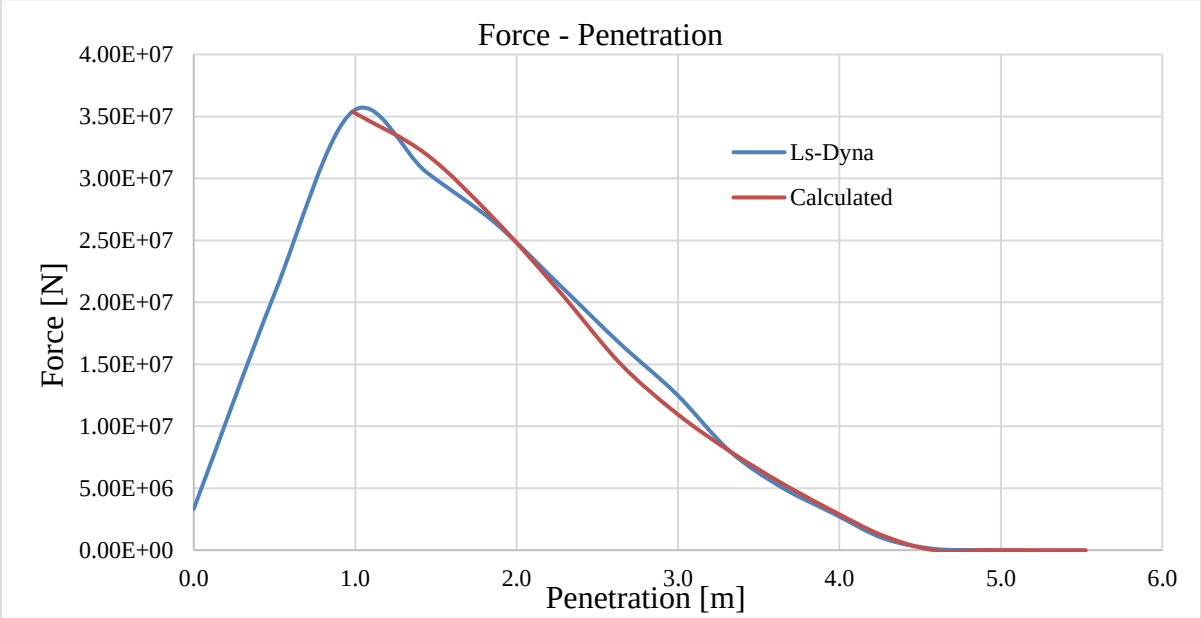

Figure 40 – Comparison of Resistance Forces for Point - 3

For Point – 3, calculated values are in the strict consistency with the ones which has been taken from Ls-Dyna. As a result, same situation is valid regarding absorbed internal energies after rupture which can be seen in the figure below.

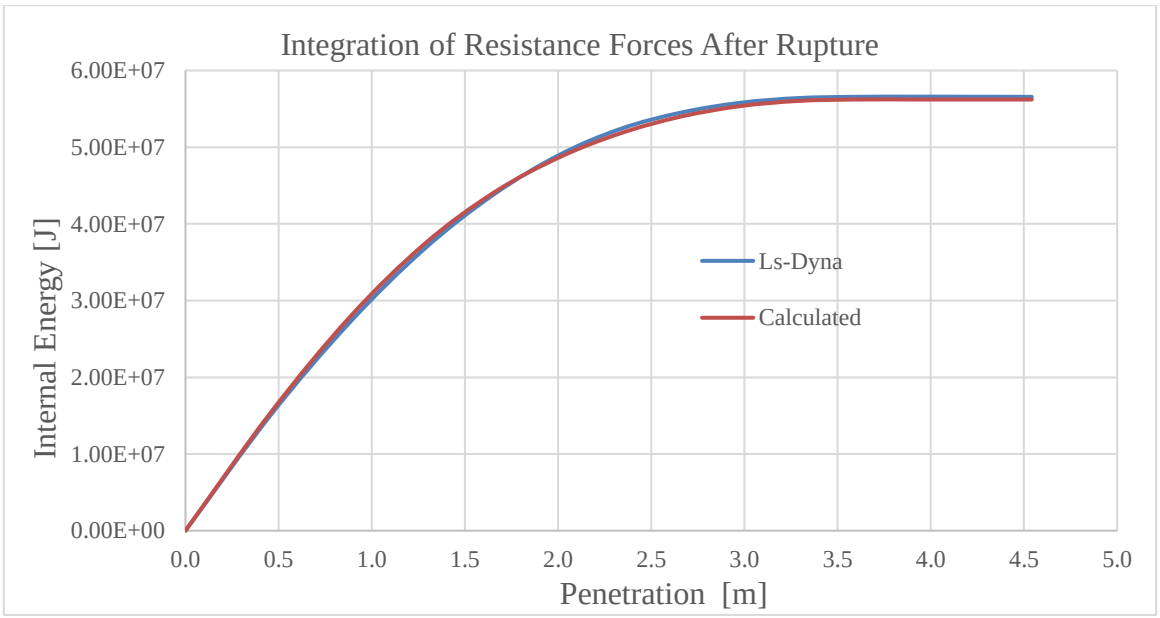

Figure 41 – Comparison of Internal Energies for Point – 3

Considering the post rupture resistant force, the discrepancy between analytical and numerical models is less than 1% , as presented in next table.

Table 6 – Discrepancy in Internal Energies for Point - 3

Absorbed Energy After Rupture (in Joules)			
By	LS-Dyna	Calculation	Discrepency
Point-1	5.67E+07	5.62E+07	0.91%

5. IMPLEMENTING THE METHOD INTO SHARP

5.1. Additional Assumptions for the Hypothesis

The proposed analytical expression to assess post-rutpture resistant force has been validated for a basic shell element. Comparisons of analytical and numerical simulations for different collision point locations and different thicknesses were presented in above sections. The discrepancies are varying between 8% and 1%. Considering these results; it can be said that the proposed method can be used to calculate post rupture resistance forces and internal energies of a shell element.

As explained above; in basic trials, sectional areas of the striking ship which represent the non-resisting areas of shell element were calculated by a 3D modelling software. Thus, it is necessary to define these areas analytically in order to implement the method in SHARP solver.

Besides in order to calculate the largest non-resisting area, final penetration which is unknown during the simulation has to be determined. To do so, an additional assumption has to be made. As expected, between the impact and the rupture moments, deceleration of the striking ship is varying. In order to evaluate the final indentation, it is assumed that the deceleration of striking ship will be constant after the rupture. In other words, the velocity of the striking ship will decrease linearly while the struck ship velocity is increasing with same trend. When both velocities are equal, simulation will stop and total penetration can be post-processed.

Thanks to that assumption, penetration can be calculated easily and thus area ratios can be used to evaluate resistance force of the side shell after rupture. Therefore the contribution of the side shell to the total internal energy can be assessed.

5.1.1. Analytical Area Calculation

In order to implement the proposed method into SHARP's code, an analytical area calculation formula is needed. Between the parallel body and the stem point, ship's section is in trapezoid shape and it can be calculated accurately. But from the stem point to bow tip, the ship section does not have a geometrically defined shape which can be seen in Figure 43.

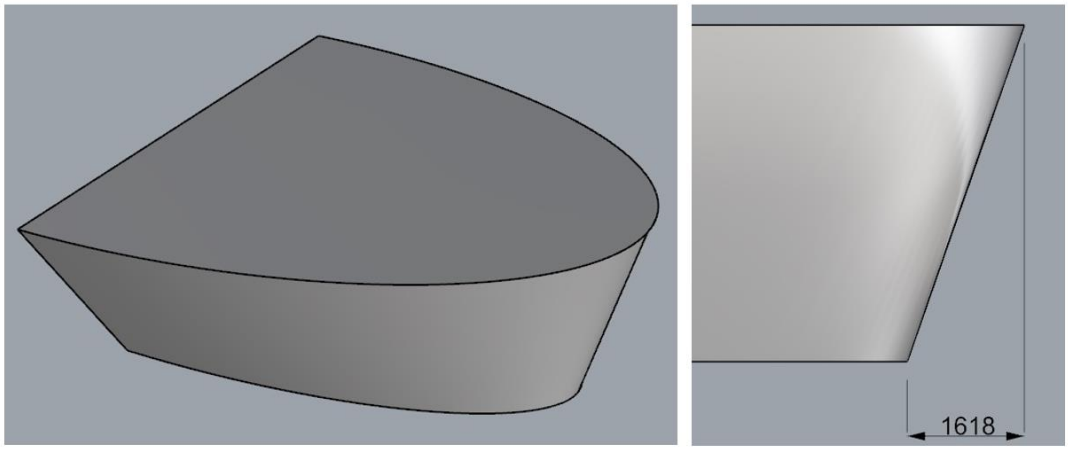

Figure 42 – Perspective and Profile View of Striking Ship

As it was mentioned in previous parts of this paper; considering ADN Regulations, all the calculations will be made until 1m of penetration. That is to say, the sectional area will not be a trapezoid for present case. Indeed, it can be said that this will be the situation for most of the cases because it is rare to have a bow shape for which the distance between the stem point and bow tip is less than 1 m.

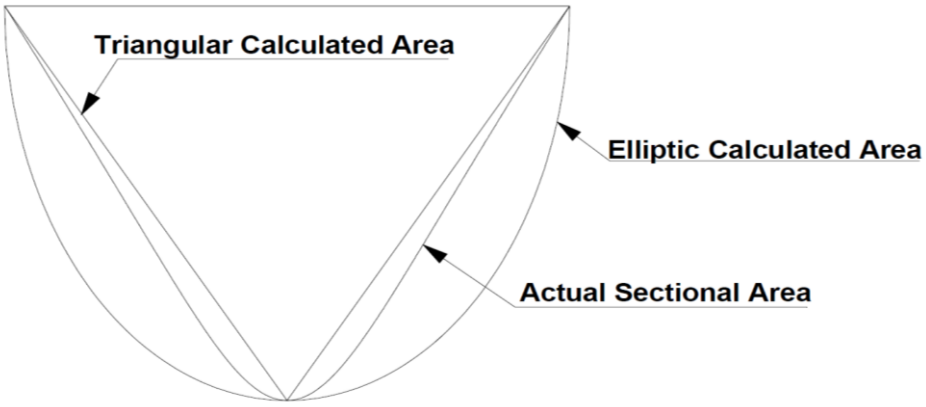

Figure 43 – Section Between Stem and Bow Tip

In Fig. 43, a transversal section of striking ship between stem point and bow tip is shown. If a triangular calculated area is used for calculating post rupture resistance, results are expected to be slightly non-conservative. As the sectional areas will be smaller than actual values, resisting area will be larger than it is. On the other hand, trapezoid areas will give conservative results but far from reality because of relatively high discrepancy. In order to compare results of both situations, simulation for Point-3 was retested with analytical formulas.

5.1.2. Triangular Calculated Sectional Areas

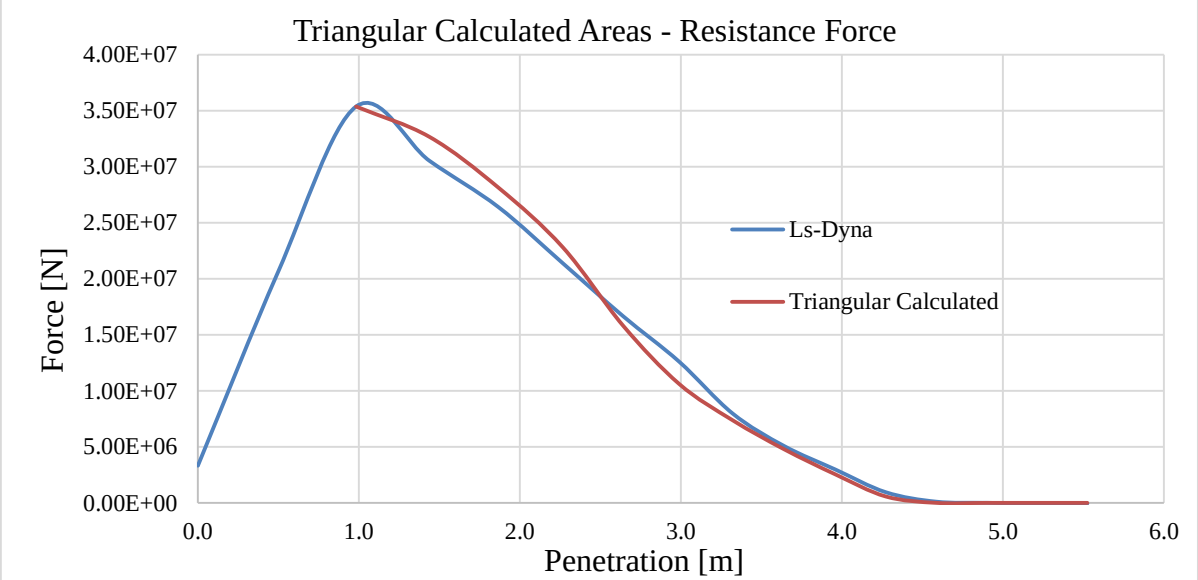

Figure 44 – Analytically Calculated Resistance Force with Triangular Areas vs Ls-Dyna Resistance Force

As expected, analytical calculated resistance force diagram shows a good correlation with finite element results. And post rupture internal energy curves obtained by integrating resistance forces are presented in the following figure.

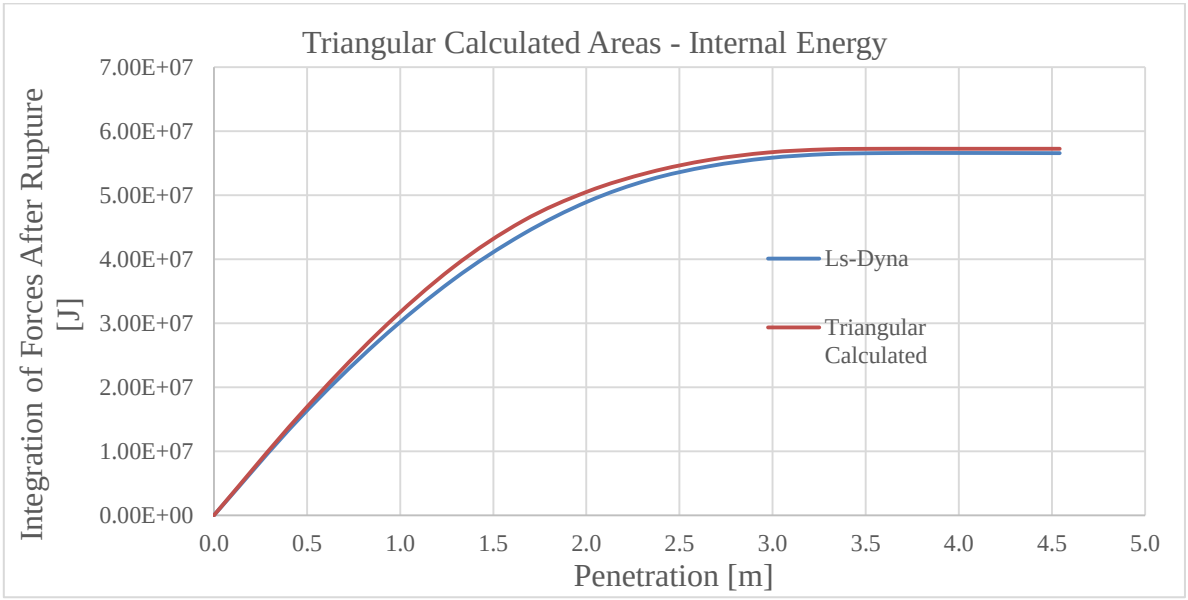

Figure 45 - Analytically Calculated Internal Energy with Triangular Areas vs Ls-Dyna Internal Energy

Total post rupture internal energy curve comparisons show that analytical calculation is not far from reality but it is not conservative any more. The discrepancy between two resulting curves can be seen in the following table.

Table 7 – Discrepancy Between Analytical Calculation with Triangular Areas and Ls-Dyna Outcomes

Absorbed Energy After Rupture (in Joules)			
By	LS-Dyna	Calculation	Discrepency
Point-3	5.67E+07	5.72E+07	- 0.91%

The discrepancy obtained in previous section, in which the areas were calculated by 3D modelling software was also around 1%, but it was conservative. Although it is not conservative any more, the results obtained with analytical calculation based on triangular areas are acceptable with -1% of discrepancy. But still, it is beneficial to test same simulation with elliptical calculated areas.

5.1.3. Elliptic Calculated Areas

It is clearly visible in Figure 43 that elliptic calculated areas will be larger than actual ones. Therefore more conservative results are expected. Moreover, as the area calculation methods differ for penetrations occuring before and after stem, around that point there may be a discontinuity regarding the evolution of sectional areas. In other words, last elliptic calculated areas can be larger than first trapezoid areas. In order to solve this issue, a constraint was used in excel spreadsheet. The trapezoid areas which are smaller than the elliptic areas are assumed to be equal maximum elliptic area. Results of the comparison can be seen in the figure below.

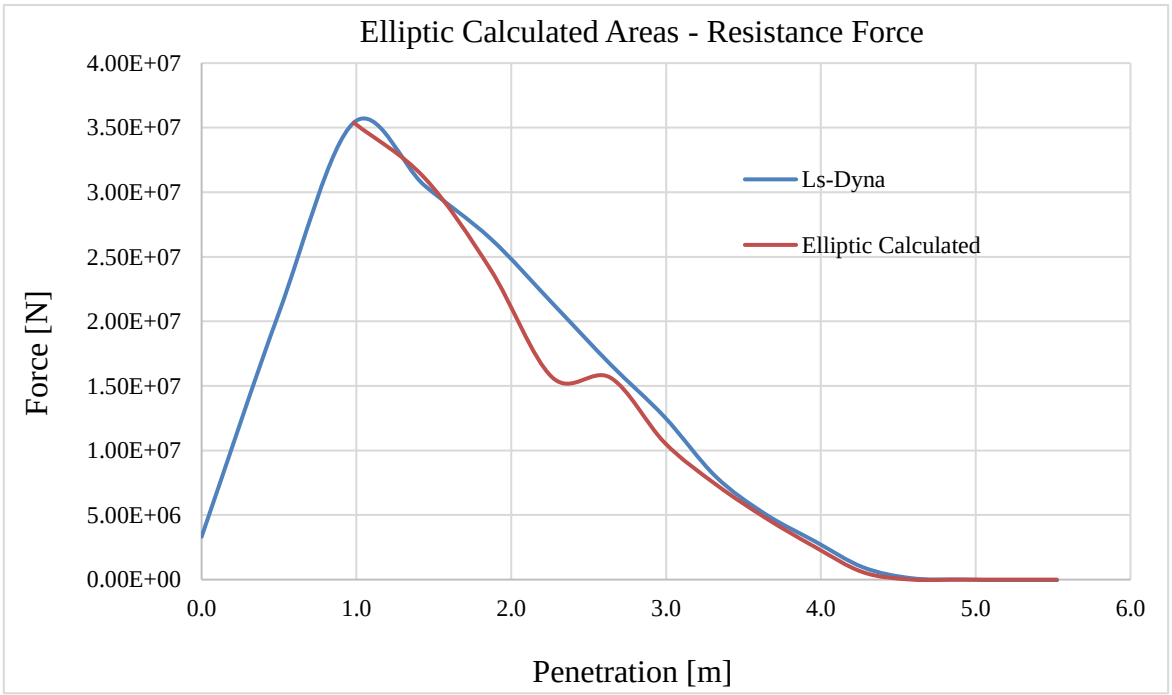

Figure 46 - Analytically Calculated Resistance Force with Elliptic Areas vs Ls-Dyna Resistance Force

Expected discontinuity is visible in Figure 46 and it is clear that calculation is conservative. In order to see it accurately, integration of resistance forces has been done and internal energy evolution is depicted in following figure.

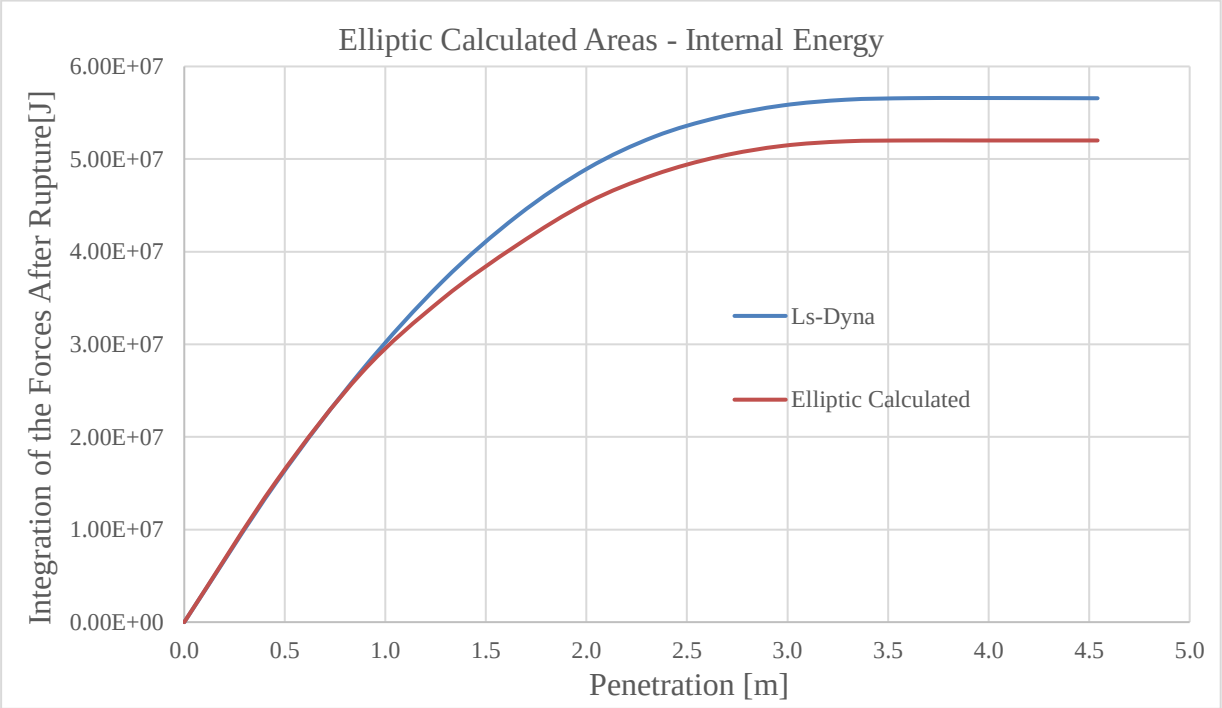

Figure 47 - Analytically Calculated Internal Energy with Elliptic Areas vs Ls-Dyna Internal Energy

The discrepancy between analytical and numerical internal energies is presented in the following table.

Table 8 - Discrepancy Between Analytical Calculation with Elliptic Areas and Ls-Dyna Outcomes

Absorbed Energy After Rupture (in Joules)			
By	LS-Dyna	Calculation	Discrepency
Point-3	5.67E+07	5.20E+07	8.33%

There is about 8% of difference between analytical calculated internal energy with elliptical areas and actual one. But it is necessary to point out that; even the result is relatively far from actual one in comparison with triangular area calculation, it is in conservative region.

Consequently, it seems to be more beneficial to calculate post rupture internal energy by using triangular areas. However; in the following sections of this thesis, while studying real ship models, both area calculation methods will be tested in order to choose the effective one more accurately.

5.2. Determining Final Penetration

An additional assumption about linear change in velocities was made above. It was assumed that the striking ship velocity will decrease linearly while struck ship one is increasing with same behaviour. Then, when surge velocity of striking ship is equal to the sway velocity of struck ship, the simulation will be stopped. This assumption will be checked with basic cases.

In basic cases, two different decelerations were compared. If the first rupture occurs in the time step of 'n'; first deceleration is the one between time step 'n-2' and 'n-1', and second value is deceleration between time step of 'n-1' and 'n'. Results of both situations were demonstrated.

5.2.1. Basic Case for Point – 1

Same basic panel which was used to test post-rupture force assessment will be used for final penetration calculation as well. Shell plate thickness was set as 50 mm for Point – 1.

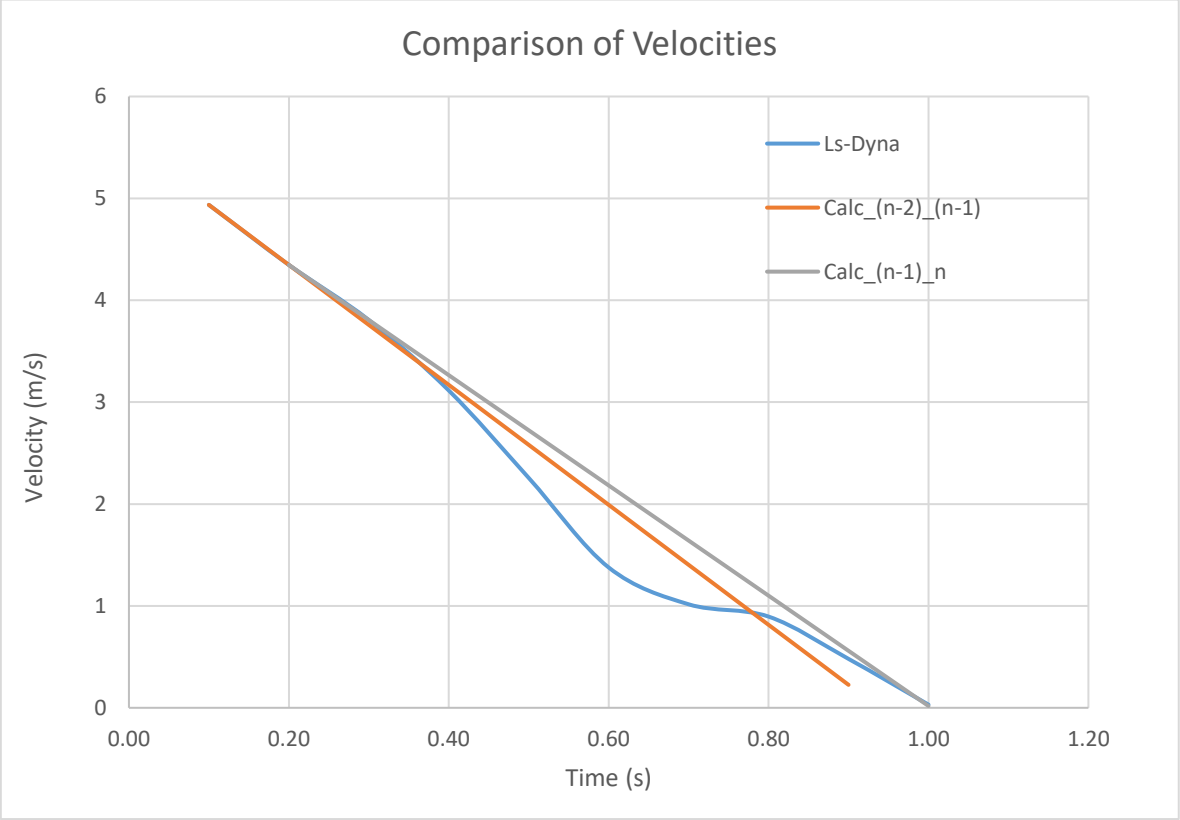

Figure 48 – Surge Velocity of Striking Ship vs Time for Point – 1

Figure 48 indicates a differentiation from 0.5 s to 0.8 seconds. Vertical movement of striking ship is a reason for that distinction. In Ls-Dyna simulations, gravity was not considered, therefore ship moves in vertical direction as well. But as a result, even the assumption is not matching perfectly with Ls-Dyna result, total penetrations are not far from each other. The deceleration between the time steps of 'n-1' and 'n' is in better accordance with Ls-Dyna results.

5.2.2. Basic Case for Point – 2

For the simulation of Point – 2, shell plate thickness was 10 mm which is relatively thin. Thus striking ship passes through the panel easily.

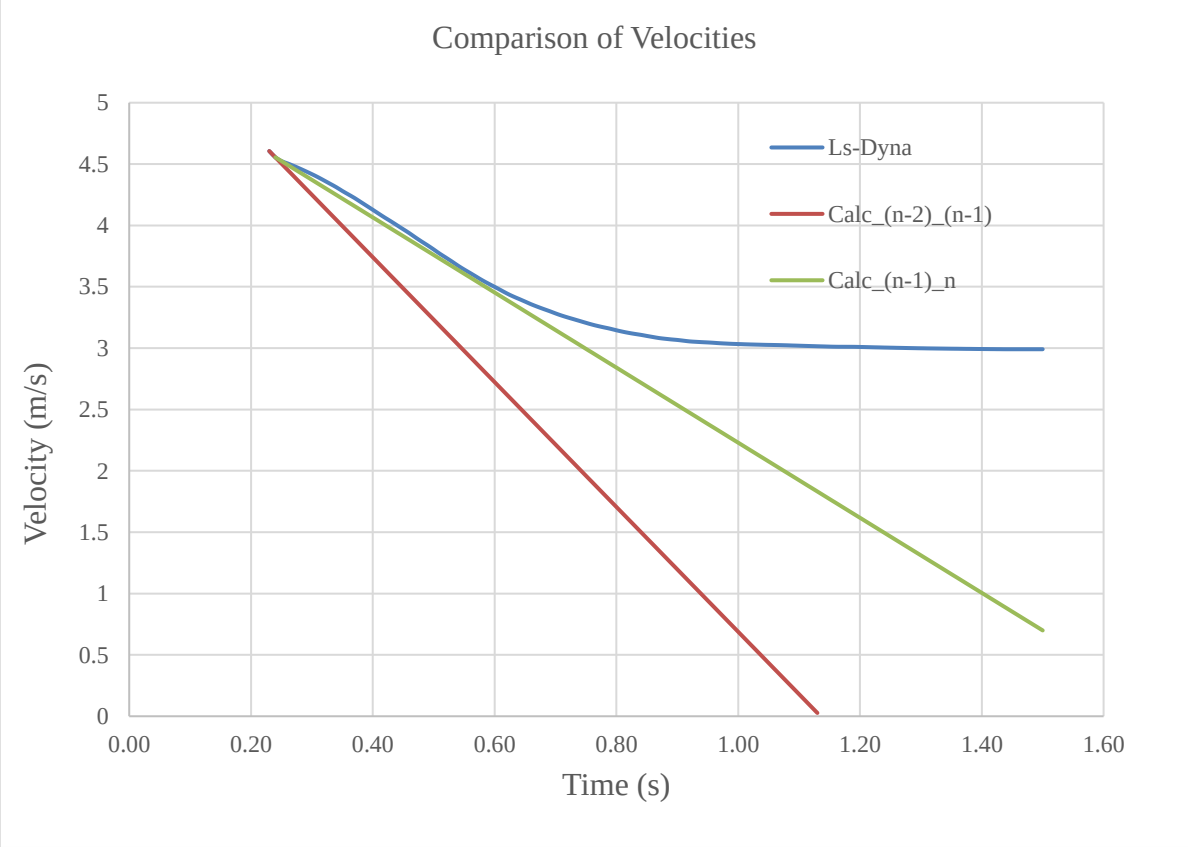

Figure 49 - Surge Velocity of Striking Ship vs Time for Point – 2

Figure 49 shows a huge difference in final velocities. This is because the striking ship passes through the clamped side shell. In order to prevent this situation to cause an enormous error, the assumption has to be improved. To do so another constraint was added to final penetration calculation. It has been said that the simulation will stop when the surge velocity of striking

ship is equal to the sway velocity of struck ship. In addition, the simulation will also stop when penetration is equal to the length of the striking bow. Under that circumstances, velocity curve of basic case related to Point – 2 will perfectly match with Ls-Dyna result, because the simulation will stop around 0.75 seconds when the non-resisting area is equal to the striking bow's largest sectional area.

As explained in previous part, for the simulation of Point 3, thin shell element was used, therefore striking ship is passing through the side shell, so velocity diagrams is expected to be same as the one related to Point – 2.

All in all; considering above explained results, by assuming that deceleration between the time steps of 'n-1' and 'n' is constant during entire simulation, final penetration can be calculated.

6. SIMULATING REAL SHIPS COLLISIONS

6.1. General Definition of the Method

In order to test the proposed expression to assess post-rupture resistance, same simulations as the ones performed by Sone Oo (2017) were used. First step of the post rupture resistance calculation is to determine maximum resistance force and collapse moment. Thanks to SHARP, this values are easily reachable.

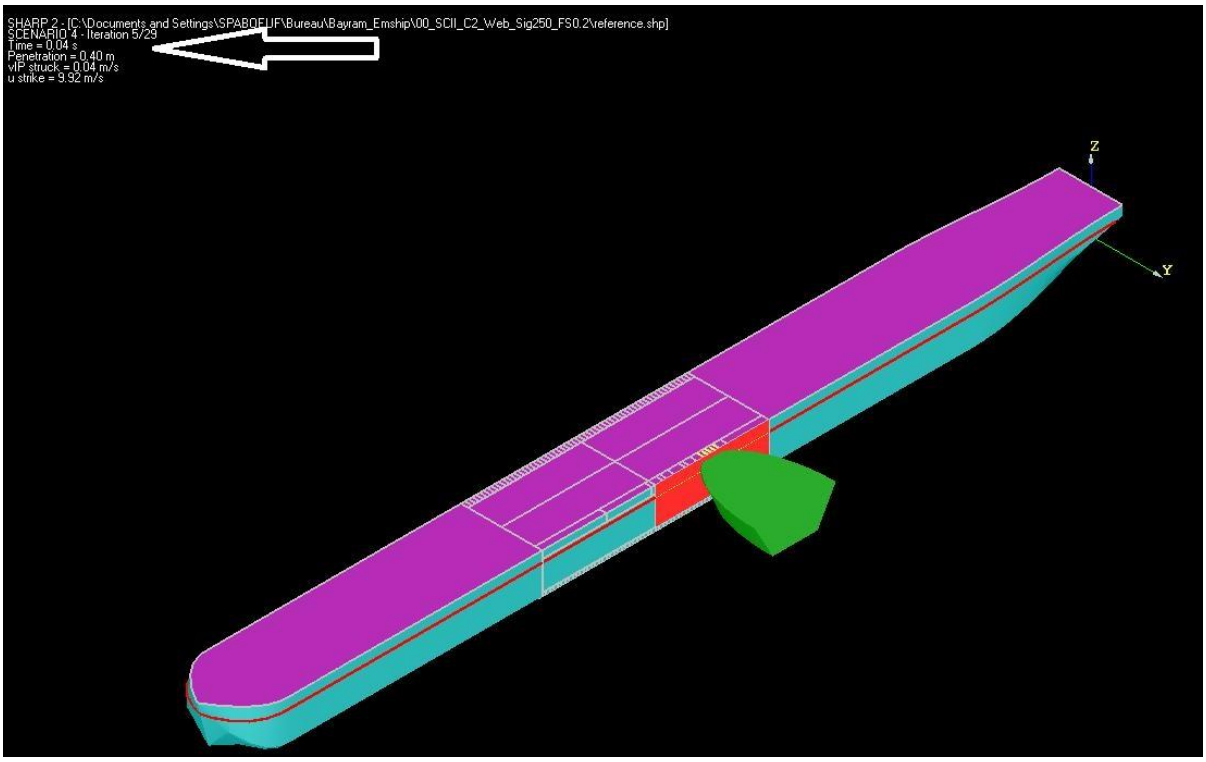

Figure 50 – Collapse Moment of SE-1

Figure 50 shows the GUI (Graphical User Interface) of the SHARP software. In SHARP, red colour represents the ruptured elements and yellow colour is for the active (impacted) elements. In this figure, collapse moment of the SE-1 can be seen and time step is shown. Also active web frames can be seen in yellow colour just in front of the striking ship.

The penetration of striking ship and velocities of both vessels at corresponding time step was given in GUI as well (upper left corner of the screen). It should be noted that both velocities are in Y direction. To state strictly, ‘u strike’ is the surge velocity of striking ship and ‘vIP Struck’ is sway velocity of the struck ship.

The collapse moment is also visible in SHARP result file 'F_STRUCK.csv' which can be seen in Figure 51.

	A	B	C	D	E	F	G
1	Time(s)	nb elts act	enfoncem	F_total	M_yaw	M_roll	F_side_shell
2	0	0	0	0	0	0	0
3	0.01	4	0.1	1.13E+07	-3.91E+07	2.35E+07	1.12E+07
4	0.02	7	0.199719	3.70E+06	-1.28E+07	7.70E+06	2.97E+06
5	0.03	11	0.299069	6.81E+06	-2.36E+07	1.42E+07	4.45E+06
6	0.04	12	0.398164	3.09E+06	-1.07E+07	6.42E+06	0
7	0.05	15	0.49702	5.23E+06	-1.81E+07	1.09E+07	0
8	0.06	17	0.59567	6.45E+06	-2.23E+07	1.34E+07	0
9	0.07	19	0.694037	8.63E+06	-2.98E+07	1.80E+07	0
10	0.08	22	0.792033	1.10E+07	-3.82E+07	2.30E+07	0
11	0.09	25	0.889552	1.39E+07	-4.82E+07	2.90E+07	0
12	0.1	25	0.986461	1.78E+07	-6.15E+07	3.70E+07	0
13	0.11	28	1.0826	1.26E+07	-4.35E+07	2.62E+07	0
14	0.12	29	1.17799	1.44E+07	-4.97E+07	2.99E+07	0
15	0.13	26	1.27273	9.54E+06	-3.30E+07	1.99E+07	0
16	0.14	28	1.36689	8.42E+06	-2.91E+07	1.75E+07	0
17	0.15	31	1.4606	7.80E+06	-2.70E+07	1.62E+07	0
18	0.16	38	1.55392	8.21E+06	-2.84E+07	1.71E+07	0
19	0.17	42	1.64684	9.74E+06	-3.37E+07	2.03E+07	0
20	0.18	46	1.73933	1.11E+07	-3.82E+07	2.30E+07	0
21	0.19	50	1.83131	6.60E+06	-2.28E+07	1.37E+07	0
22	0.2	56	1.92286	5.65E+06	-1.95E+07	1.18E+07	0

Figure 51 – Collapse Moment and Max Resistance Force of SE-1

In same file, maximum resistance forces of all elements can be seen. In this example, maximum resistance force of side shell is highlighted by a red circle and that force will be used as 'F_{Max}' in proposed formula. Then the final penetration has to be calculated. To do so, deceleration of the striking ship and acceleration of the struck ship has to be calculated between 0.03 and 0.04 time steps for this particular case. In Figure 52 velocities of both vessels, are highlighted (red rectangles) as well as related time steps (red underlines).

2 0.2000E-01 0.0000E+00 0.5202E+00 0.0000E+00 0.7912E-01 0.0000E+00 -0.1685E-02 0.0000E+00 0.1616E-01 0.0000E+00 0.2458E-02
0.1915E-11 -0.4812E-06 -0.7036E+01 0.0000E+00 -0.3305E+03 0.0000E+00 -0.8650E+03 0.0000E+00 0.0000E+00 -0.6677E+03 0.0000E+00 0.
0.0000E+00 0.0000E+00 0.0000E+00 0.0000E+00 0.0000E+00 -0.8152E-02 -0.2078E+04 -0.4495E-01 0.0000E+00 0.1340E+06 0.0000E+00 0.
0.0000E+00 -0.2447E+07 0.0000E+00 0.4743E+07 0.1886E+05 0.0000E+00 0.4281E+07 0.0000E+00 0.1387E+08 0.0000E+00 0.0000E+00 -0
0.0000E+00 0.1378E+08 0.0000E+00 0.4408E+10 0.0000E+00 0.0000E+00 0.4749E+07 0.0000E+00 0.1761E+08 0.0000E+00 0.4715E+10 -0
0.0000E+00 0.0000E+00 0.0000E+00
1 0.3000E-01 -0.2173E+01 -0.6010E-03 -0.1175E+00 -0.5138E-04 -0.1348E-01 -0.1975E-03 0.9937E+01 -0.1755E-04 -0.3390E-02 -0.1406E-05 -
0.3985E-05 -0.8606E-07 -0.6542E+03 0.1723E+03 -0.1187E+05 -0.2830E+03 -0.1626E+08 0.1808E+04 0.1267E+03 -0.5889E+00 0.7211E+03 -0.
0.0000E+00 0.0000E+00 0.0000E+00 0.0000E+00 0.0000E+00 0.3815E+03 0.5354E+00 0.2622E+05 0.0000E+00 0.9984E+05 0.0000E+00 0
0.0000E+00 0.8770E+06 0.0000E+00 0.2608E+08 -0.4245E+06 0.0000E+00 0.2472E+07 0.0000E+00 -0.5520E+08 0.0000E+00 0.0000E+00 0
0.0000E+00 0.8012E+08 0.0000E+00 0.9413E+09 0.0000E+00 0.0000E+00 -0.1395E+08 0.0000E+00 -0.9729E+07 0.0000E+00 0.1039E+10 0
0.0000E+00 0.0000E+00 0.0000E+00
2 0.3000E-01 -0.1674E-05 0.7933E+00 -0.5670E-04 0.1207E+00 -0.1206E-06 -0.2569E-02 -0.8371E-08 0.2273E-01 -0.2835E-06 0.3457E-02 -0
0.2401E-10 -0.1111E-05 -0.1392E+02 -0.1131E-01 -0.6538E+03 0.2102E-01 -0.1711E+04 0.2935E-01 0.8341E-04 -0.1541E+04 0.6113E-02 0.706
+00 0.0000E+00 0.0000E+00 0.0000E+00 0.0000E+00 -0.9555E-01 -0.4797E+04 -0.5525E+00 0.0000E+00 0.1339E+06 0.0000E+00 0.2412E+
0.2446E+07 0.0000E+00 0.4741E+07 0.1885E+05 0.0000E+00 0.4280E+07 0.0000E+00 0.1386E+08 0.0000E+00 0.0000E+00 -0.2505E+07 0
0.1377E+08 0.0000E+00 0.4407E+10 0.0000E+00 0.0000E+00 0.4747E+07 0.0000E+00 0.1760E+08 0.0000E+00 0.4712E+10 -0.1639E+00 0
0.0000E+00 0.0000E+00
1 0.4000E-01 -0.1143E+01 -0.2953E-03 -0.7720E-01 -0.3106E-04 -0.1043E-01 -0.1032E-03 0.9920E+01 -0.2203E-04 -0.4363E-02 -0.1818E-05 -0
0.1056E-04 -0.1505E-06 -0.8510E+03 0.2175E+03 -0.1541E+05 -0.3561E+03 -0.1620E+08 0.2282E+04 0.2219E+03 -0.1034E+01 0.1269E+04 -0.
0.0000E+00 0.0000E+00 0.0000E+00 0.0000E+00 0.0000E+00 0.6684E+03 0.9492E+00 0.4625E+05 0.0000E+00 0.9976E+05 0.0000E+00 0
0.0000E+00 0.8758E+06 0.0000E+00 0.2606E+08 -0.4242E+06 0.0000E+00 0.2471E+07 0.0000E+00 -0.5517E+08 0.0000E+00 0.0000E+00 0
0.0000E+00 0.8009E+08 0.0000E+00 0.9409E+09 0.0000E+00 0.0000E+00 -0.1396E+08 0.0000E+00 -0.9719E+07 0.0000E+00 0.1038E+10 0
0.0000E+00 0.0000E+00 0.0000E+00
2 0.4000E-01 -0.2687E-05 0.4191E+00 -0.9101E-04 0.6373E-01 -0.1936E-06 -0.1357E-02 -0.3017E-07 0.2879E-01 -0.1022E-05 0.4379E-02 -0.
10 -0.1945E-05 -0.2234E+02 -0.5164E-01 -0.1049E+04 0.9598E-01 -0.2746E+04 0.1340E+00 0.4675E-03 -0.2699E+04 0.3426E-01 0.1236E+04
0.0000E+00 0.0000E+00 0.0000E+00 0.0000E+00 -0.2688E+00 -0.8399E+04 -0.1626E+01 0.0000E+00 0.1338E+06 0.0000E+00 0.2410E+05 0
0.2444E+07 0.0000E+00 0.4737E+07 0.1884E+05 0.0000E+00 0.4279E+07 0.0000E+00 0.1385E+08 0.0000E+00 0.0000E+00 -0.2503E+07 0
0.1376E+08 0.0000E+00 0.4405E+10 0.0000E+00 0.0000E+00 0.4743E+07 0.0000E+00 0.1758E+08 0.0000E+00 0.4708E+10 -0.3636E+00 0
0.0000E+00 0.0000E+00
1 0.5000E-01 -0.1500E+01 -0.3939E-03 -0.9148E-01 -0.3949E-04 -0.1144E-01 -0.1349E-03 0.9907E+01 -0.2548E-04 -0.5206E-02 -0.2171E-05 -0
0.1628E-04 -0.2284E-06 -0.1031E+04 0.2532E+03 -0.1864E+05 -0.4133E+03 -0.1616E+08 0.2655E+04 0.3388E+03 -0.1575E+01 0.1950E+04 -0.
0.0000E+00 0.0000E+00 0.0000E+00 0.0000E+00 0.0000E+00 0.1019E+04 0.1461E+01 0.7132E+05 0.0000E+00 0.9965E+05 0.0000E+00 0
0.0000E+00 0.8744E+06 0.0000E+00 0.2605E+08 -0.4239E+06 0.0000E+00 0.2470E+07 0.0000E+00 -0.5513E+08 0.0000E+00 0.0000E+00 0
0.0000E+00 0.8004E+08 0.0000E+00 0.9404E+09 0.0000E+00 0.0000E+00 -0.1396E+08 0.0000E+00 -0.9705E+07 0.0000E+00 0.1037E+10 0

Figure 52 – Velocities of Both Vessels for Related Time Steps

External dynamic calculations of SHARP are written in result MCOL file ‘mcol.txt’ which can be seen in Figure 52. In this file, striking ship is called as Ship – 1 and struck ship is Ship – 2. Related time steps and corresponding velocities are emphasized in same figure.

The velocities that were written in ‘mcol.txt’ file are calculated according to center of gravity of the vessel. In reality it should be calculated with the velocities at collision point, because yaw or roll movement of the ship may occur. But in this case, center of gravity is very close to the collision point, so yaw and roll movements of the struck ship are sufficiently small to be neglected.

	A	B	C	D	E	F	G	H	I	J	K	L
1												
2	$V_{striking}$ (n-1)	9.9981	m/s		Time	$V_{Striking}$	V_{struck}	Penet After Rup	Sec Area (m^2)	Area Ratio	Res Force (N)	Energy (J)
3	$V_{striking}$ n	9.955	m/s		0.020	9.998	0.007	0.000	0.00	0.000	4.46E+06	0
4	V_{struck} (n-1)	0.006779	m/s		0.030	9.955	0.016	0.000	0.00	0.000	4.46E+06	0.00E+00
5	V_{struck} (n)	0.01616	m/s		0.040	9.912	0.026	0.099	0.21	0.005	4.44E+06	4.40E+05
6	Rupture Moment	0.04	s		0.050	9.869	0.035	0.197	0.58	0.015	4.40E+06	8.74E+05
7	Time Step	0.01	s		0.060	9.826	0.044	0.295	1.06	0.027	4.34E+06	1.30E+06
8					0.070	9.783	0.054	0.392	1.63	0.041	4.28E+06	1.72E+06
9	Final Area	40.05	m^2		0.080	9.740	0.063	0.489	2.26	0.057	4.21E+06	2.13E+06
10	Max Force	4.46E+06	N		0.090	9.696	0.072	0.585	2.96	0.074	4.13E+06	2.53E+06
11					0.100	9.653	0.082	0.681	3.70	0.092	4.05E+06	2.92E+06
12					0.110	9.610	0.091	0.776	4.50	0.112	3.96E+06	3.30E+06
13					0.120	9.567	0.101	0.871	5.33	0.133	3.87E+06	3.68E+06
14					0.130	9.524	0.110	0.965	6.21	0.155	3.77E+06	4.03E+06
15					0.140	9.481	0.119	1.059	7.12	0.178	3.67E+06	4.38E+06
16					0.150	9.438	0.129	1.152	8.06	0.201	3.56E+06	4.72E+06
17					0.160	9.395	0.138	1.244	9.04	0.226	3.45E+06	5.04E+06
18					0.170	9.352	0.147	1.336	10.04	0.251	3.34E+06	5.36E+06
183					1.820	2.240	1.695	9.336	40.03	0.999	2.49E+03	1.33E+07
184					1.830	2.197	1.705	9.341	40.03	1.000	2.01E+03	1.33E+07
185					1.840	2.154	1.714	9.345	40.03	1.000	1.58E+03	1.33E+07
186					1.850	2.111	1.724	9.349	40.04	1.000	1.20E+03	1.33E+07
187					1.860	2.068	1.733	9.352	40.04	1.000	8.79E+02	1.33E+07
188					1.870	2.025	1.742	9.355	40.04	1.000	6.05E+02	1.33E+07
189					1.880	1.981	1.752	9.357	40.04	1.000	3.82E+02	1.33E+07
190					1.890	1.938	1.761	9.359	40.05	1.000	2.10E+02	1.33E+07
191					1.900	1.895	1.770	9.361	40.05	1.000	8.94E+01	1.33E+07
192					1.910	1.852	1.780	9.361	40.05	1.000	1.93E+01	1.33E+07
193					1.920	1.809	1.789	9.361	40.05	1.000	0.00E+00	1.33E+07

Figure 53 – Final Penetration Calculation

The related velocities of both vessels are changing linearly. In other words, surge velocity of the striking ship is decreasing with the deceleration between the time steps of ‘n-1’ and ‘n’, while the sway velocity of struck ship is increasing with the acceleration in same time steps. And penetration is calculated by integration of movement in all time steps. Penetration in one time step is equal to relative velocity multiplied by time step. In the example which is demonstrated in Figure 53, simulation was stopped because the striking and struck ships velocities were equal and total penetration after rupture was 9.3 m. The length of the striking bow model is 12 m, so it can be said that the striking ship did not pass through the side shell of the struck ship.

As explained above, there are two conditions to stop the simulation. First one is; the surge velocity of striking ship is equal or less to the sway velocity of struck ship. Even if there is still movement, striking ship cannot apply any force to struck ship under that circumstances. Second condition is; total penetration is equal to the length of the striking ship bow. It means the striking ship passed to other side of the shell element, so there is no resistance any more.

Sectional area calculation can also be seen in Figure 53. Sectional areas of striking ship were calculated for each time step. These areas are assumed to be equal to non-resisting area of shell element. Thus resistance force for each time step can be estimated proportionally to the resisting area of shell element.

Thereafter, resistance forces were integrated in order to calculate post rupture internal energy of the side shell for each time step.

Table 9 – Example for Internal Energy Calculation

Disp-Energy (SHARP)		Additional Post Rupture Energy (J)	Total Internal Energy
Penetration (m)	Energy (J)		
0.0	0.00E+00		0.00E+00
0.1	5.61E+05		5.61E+05
0.2	1.28E+06		1.28E+06
0.3	1.77E+06		1.77E+06
0.4	1.98E+06	4.13E+05	2.40E+06
0.5	2.27E+06	8.17E+05	3.08E+06
0.6	2.65E+06	1.21E+06	3.85E+06
0.7	3.13E+06	1.59E+06	4.72E+06
0.8	3.69E+06	1.96E+06	5.65E+06
0.9	4.41E+06	2.31E+06	6.73E+06
1.0	5.33E+06	2.66E+06	7.99E+06
1.1	6.47E+06	2.99E+06	9.47E+06

It is known that until the instant of rupture, SHARP is adding the internal energy of the side shell element to total internal energy. But after the rupture moment, there is no contribution by side shell element. So that integrated post rupture resistance forces which represent the internal energies for each time step, is added to total internal energy after the rupture instant.

6.2. Nine Different Scenarios for Each Simulation

As explained before, in SHARP each element is activated after contact with striking ship. In Figure 54, active and failed elements can be seen. The web frames and inner side plate which are in red colour are failed elements and all others which are in yellow colour are active (impacted) elements. Striking ship is in green colour and is defined as a rigid body.

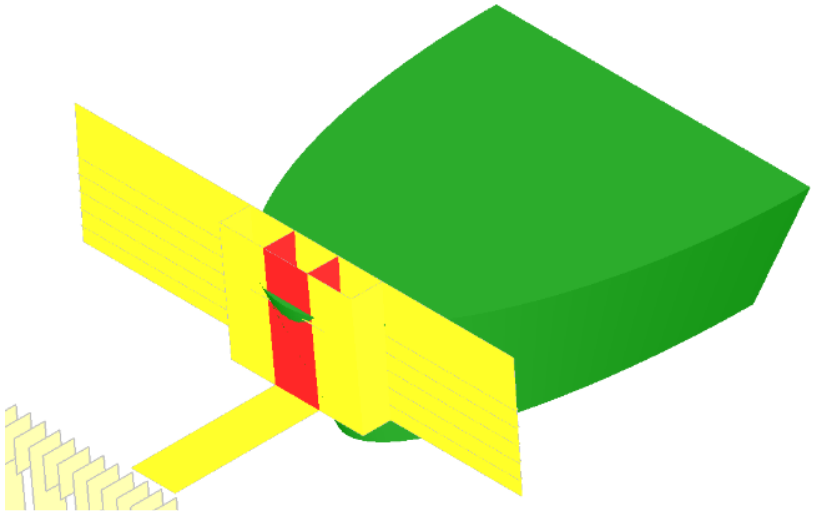

Figure 54 – Example for Activated and Failed Elements in SHARP

Because of this definition, in SHARP nine different scenarios were used to simulate a collision case. By doing so, the elements around collision point are activated in different scenarios and at the end of the simulation, average of all scenarios is being used as final result. Collision points for different scenarios can be seen in Figure 21.

Point – 1 in Figure 21 is real collision point which is wanted to be evaluated. Positions of other points are determined according to frame space and stiffner space. The points which are on left and right side of the collision point are used to activate the other web frames and side plates which are positioned next to collision point. Likewise in the collision scenarios on the points which are above and below the collision points, longitudinal stiffners and side plates around the real collision point are active. In the end of nine simulations, average of all of those was calculated to compare with finite element results. As expected; collapse moment, maximum side shell resistance force and velocities of both vessels are different in all these scenarios.

Therefore; in order to calculate average internal energy, new hypothesis is needed to be implemented to all those simulations.

Table 10 – Existing Results for Collision Case - 1

Scenario No	U_{total}@0.988 m (MJ)	$U_{SideShell}$@0.988m (MJ)	Max Side Shell Resistance (N)	Collapse Time (s)
Scenario 1	4.83E+06	1.26E+06	2.15E+06	8.00E-02
Scenario 2	4.90E+06	1.26E+06	2.15E+06	8.00E-02
Scenario 3	5.32E+06	1.64E+06	4.46E+06	3.00E-02
Scenario 4	5.33E+06	1.64E+06	4.45E+06	3.00E-02
Scenario 5	5.33E+06	1.64E+06	4.46E+06	3.00E-02
Scenario 6	4.90E+06	1.26E+06	2.15E+06	8.00E-02
Scenario 7	4.51E+06	6.40E+05	2.15E+06	9.00E-02
Scenario 8	4.33E+06	6.40E+05	2.15E+06	9.00E-02
Scenario 9	4.49E+06	6.40E+05	2.15E+06	9.00E-02

An example table is shown in Table 10. This table indicates that there are three groups which are shown in different colours. Instead of implementing the method for all nine scenarios, one scenario from each group will be chosen and average of these three will be used as final result.

Table 11 - Existing Results for Collision Case - 2

Scenario No	U_{total}@0.996 m (MJ)	$U_{SideShell}$@0.996m (MJ)	Max Side Shell Resistance (N)	Collapse Time (s)
Scenario 1	9.94E+05	6.46E+05	4.31E+06	5.00E-02
Scenario 2	1.00E+06	6.45E+05	4.31E+06	5.00E-02
Scenario 3	8.14E+05	5.91E+05	3.94E+06	5.00E-02
Scenario 4	8.20E+05	5.92E+05	3.95E+06	5.00E-02
Scenario 5	8.18E+05	5.93E+05	3.95E+06	5.00E-02
Scenario 6	1.00E+06	6.47E+05	4.31E+06	5.00E-02
Scenario 7	1.04E+06	7.41E+05	4.94E+06	5.00E-02
Scenario 8	1.05E+06	7.40E+05	4.93E+06	5.00E-02
Scenario 9	1.04E+06	7.39E+05	4.93E+06	5.00E-02

Same situation was present for Case 2 as well. Because of that, scenarios of 5, 6, 7, were chosen for both collision cases.

There is another significant point in this tables which is collapse moments. For Case 1, except for scenario 5, collapse moment is almost at 1m of penetration. But for Case 2, rupture occurs at 0.05 seconds which means less than 0.5 m of penetration. As a result, the influence of the post rupture resisance is expected to be higher for Case 2.

7. RESULTS OF COLLISION CASES

7.1. Collision Case 1

Collision point just below the weather deck of the struck ship for this case which can be seen in Figure 55. And all three scenarios were calculated with $\delta_{Rupture}$, δ_{Total} and also triangular calculated areas and elliptic calculated areas.

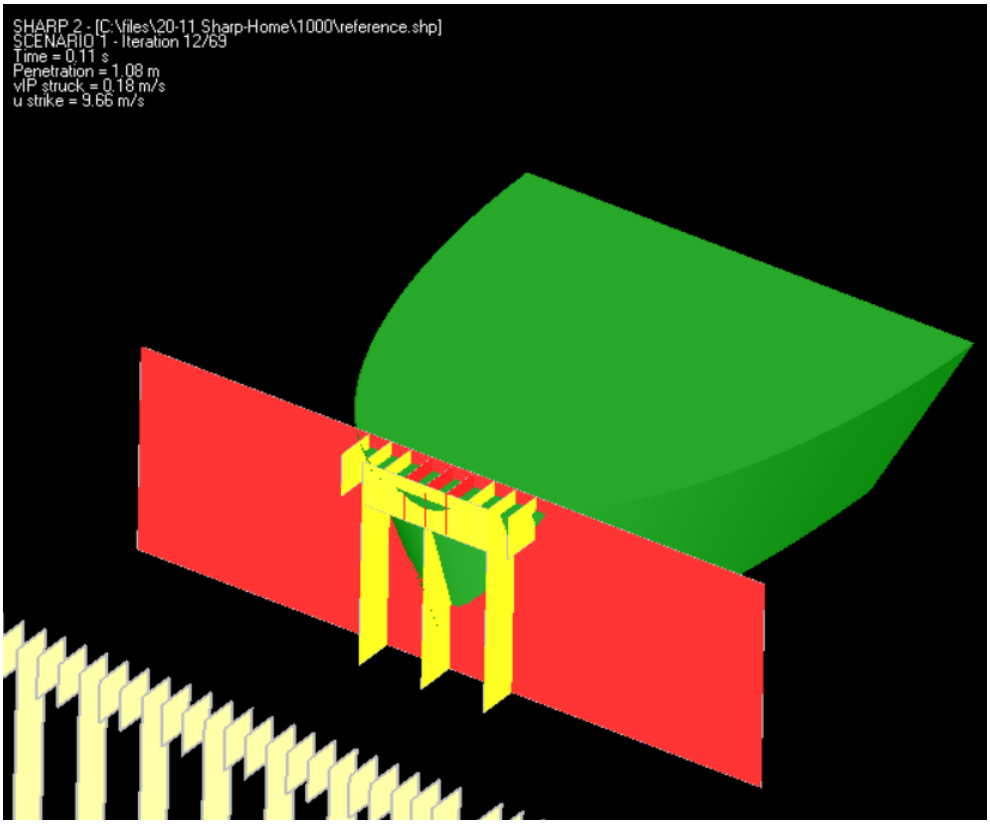

Figure 55 – 1 m of Penetration Moment for Case 1

In Figure 55, the time step where penetration exceeds 1 m is shown. Longitudinal bulkhead is activated and entire side shell seems to be failed. Post rupture resistance included results can be seen in the tables below.

Table 12 - Discrepancy in Internal Energy for Case 1 – Condition 1

Case 1 - 1 m Indentation - Average - Triangular- $\delta_{Rupture}$		
		Discre
Ls dyna	5.79E+06	-
SHARP Zero Post Rupture Resistance	5.03E+06	13.1%
SHARP with Calculated Post Rupture Resistance	6.32E+06	-9.2%

Negative sign indicates that results are not conservative anymore. For triangular calculated areas with $\delta_{Rupture}$, the discrepancy is around -9%.

Table 13 - Discrepancy in Internal Energy for Case 1 – Condition 2

Case 1 - 1 m Indentation - Average - Triangular- δ_{Total}		
		Discre
Ls dyna	5.79E+06	-
SHARP Zero Post Rupture Resistance	5.03E+06	13.1%
SHARP with Calculated Post Rupture Resistance	6.23E+06	-7.7%

In Table 13, the results of the same case which were calculated with δ_{Total} is shown and discrepancy is around -8% (non-conservative).

Table 14 - Discrepancy in Internal Energy for Case 1 – Condition 3

Case 1 - 1 m Indentation - Average - Elliptic- $\delta_{Rupture}$		
		Discre
Ls dyna	5.79E+06	-
SHARP Zero Post Rupture Resistance	5.03E+06	13.1%
SHARP with Calculated Post Rupture Resistance	6.30E+06	-8.8%

Table 14 demonstrates the discrepancies when post rupture resistance is calculated with elliptic areas and $\delta_{Rupture}$. The discrepancy is then about -9%.

Table 15 - Discrepancy in Internal Energy for Case 1 – Condition 4

Case 1 - 1 m Indentation - Average - Elliptical- δ_{Total}		
		Discre
Ls dyna	5.79E+06	-
SHARP Zero Post Rupture Resistance	5.03E+06	13.1%
SHARP with Calculated Post Rupture Resistance	6.16E+06	-6.4%

The least discrepancy for Case – 1 is in the calculation which was done by using elliptic calculated areas and δ_{Total}. It is -6%.

All in all, the discrepancies for all conditions are less than 10% but none of them are conservative.

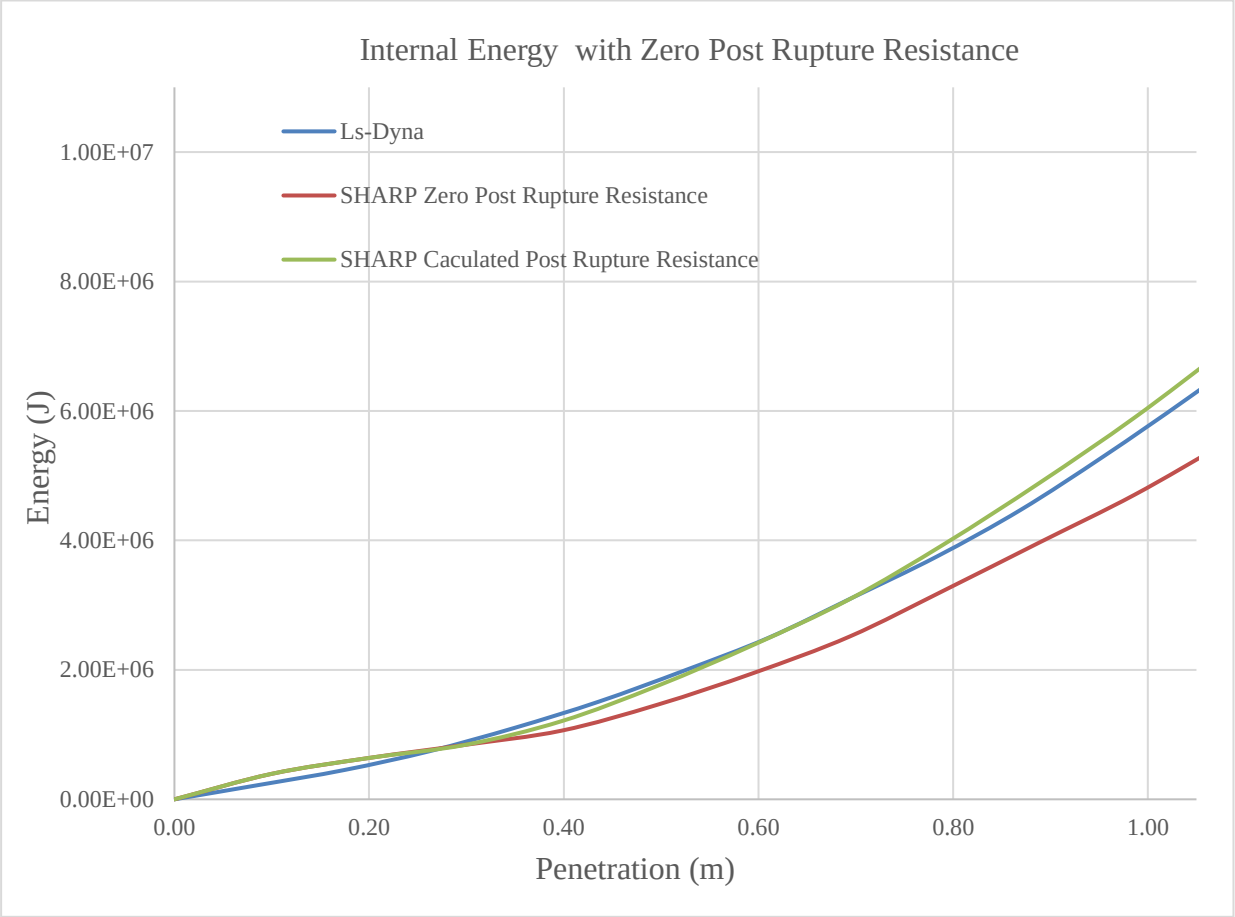

Figure 56 – Total Internal Energy Diagram for Case 1 – Condition 1

Total internal energy diagram for Case 1 can be seen in Figure 56. The influence of the post rupture resistance is recognizable after 0.3 m of penetration. This is the collapse moment of side shell in Scenario 5 for that case. As it has been shown in Table 10, for scenario 6 and 7 collapse moment is quite late. As a result, influence of the post rupture energy is relatively less for this scenario.

In order to decide the best calculation method, it is necessary to check the results for other collision cases. It should be noted here that for Case 2 in which the collision point was close to mid-depth of the struck ship, the discrepancy between LS-DYNA and SHARP results was about 80%. Thus same calculations have to be made for that case before deciding the effective method.

7.2. Collision Case 2

The collision point for Case – 2 is around mid-depth of the struck ship. The allignment of the both vessels can be seen in Figure 24. 1 m of penetration moment is shown in following figure.

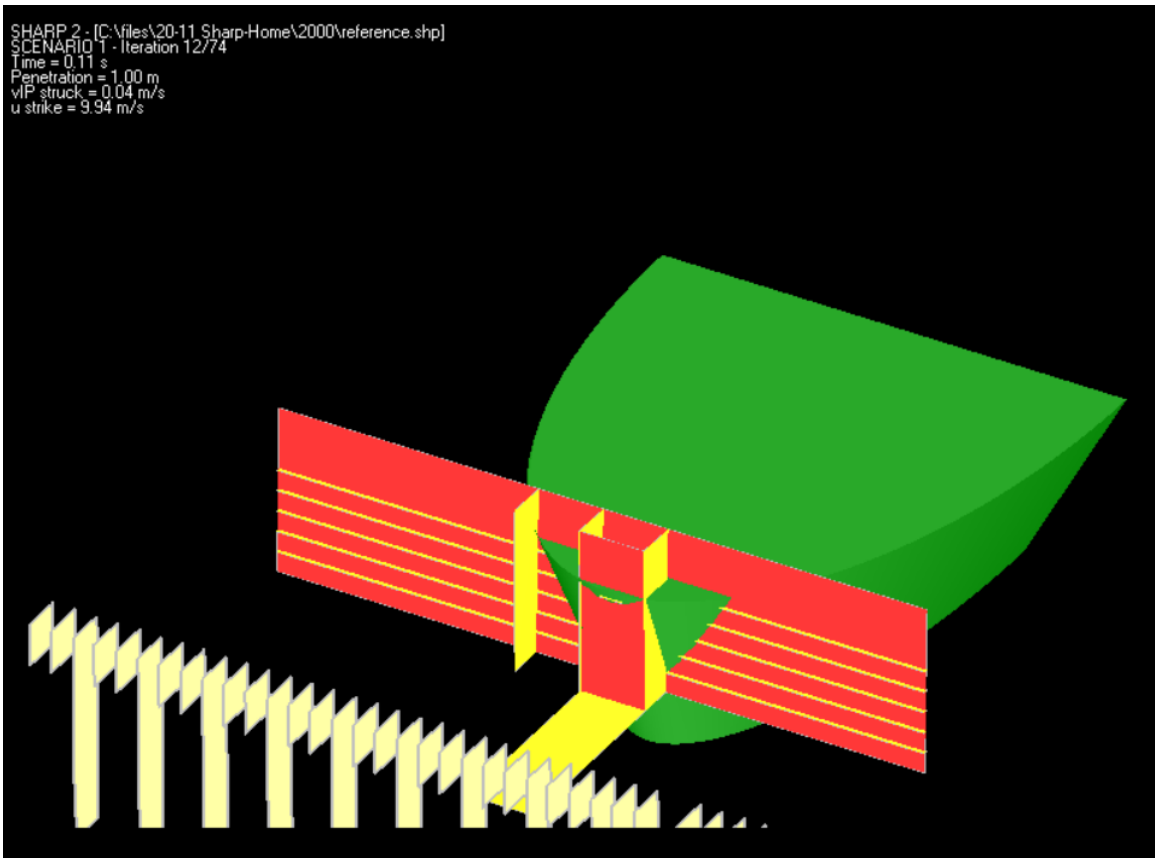

Figure 57 – 1 m of Penetration Moment for Case 2

For this case, stiffners and bottom plate is active as well. It should be remarked that longitudinal bulkhead seems to be ruptured. It is also represented by super-element 1. But in this part, post rupture behaviour for that element was not included (this will be done when implementing all the developments in SHARP solver). Post rupture internal energies were calculated for all four conditions and results are shown in the following tables.

Table 16 - Discrepancy in Internal Energy for Case 2 – Condition 1

Case 2- 1 m Indentation - Average - Triangular - $\delta_{Rupture}$		
		Discre
Ls dyna	4.49E+06	-
SHARP Zero Post Rupture Resistance	1.05E+06	76.6%
SHARP with Calculated Post Rupture Resistance	3.52E+06	21.6%

It appears that taking into account the post rupture resistance allows for significant improvement for this case. As it is shown in Table 16, the discrepancy has dropped from 77% to 22% for the calculation made with triangular calculated areas and $\delta_{Rupture}$.

Table 17 - Discrepancy in Internal Energy for Case 2 – Condition 2

Case 2 - 1 m Indentation - Average - Triangular - δ_{Total}		
		Discre
Ls dyna	4.49E+06	-
SHARP Zero Post Rupture Resistance	1.05E+06	76.6%
SHARP with Calculated Post Rupture Resistance	3.35E+06	25.5%

As it is so for previous case, in calculation with δ_{Total} , additional energy is less and, as shown in Table 17, discrepacy with LS-DYNA results increases slightly up to 25.5%.

Table 18 - Discrepancy in Internal Energy for Case 2 – Condition 3

Case 2 - 1 m Indentation - Average - Elliptic - $\delta_{Rupture}$		
		Discre
Ls dyna	4.49E+06	-
SHARP Zero Post Rupture Resistance	1.05E+06	76.6%
SHARP with Calculated Post Rupture Resistance	3.48E+06	22.5%

In Table 18, the discrepancies for Condition 3 has been shown. By Condition 3, it is meant to define the calculation which was made with elliptic calculated areas and $\delta_{Total.}$ Resulting discrepancy is about 23%.

Table 19 - Discrepancy in Internal Energy for Case 2 – Condition 4

Case 2 - 1 m Indentation - Average - Elliptic - δ_{Total}		
		Discre
Ls dyna	4.49E+06	-
SHARP Zero Post Rupture Resistance	1.05E+06	76.6%
SHARP with Calculated Post Rupture Resistance	3.23E+06	28.1%

In the calculation with elliptic areas and δ_{Total} the discrepancy is 28.1% which is the highest for Case – 2.

As expencted; influences of post rupture resistance for all conditions are higher than the ones for Case 1. This is because of the collapse moment. For Case 1, only in scenario 5, side shell failed rapidly but for Case 2, side shell fails around 0.5 m for all scenarios. Thus the influence of the post rupture resistance is quite significant.

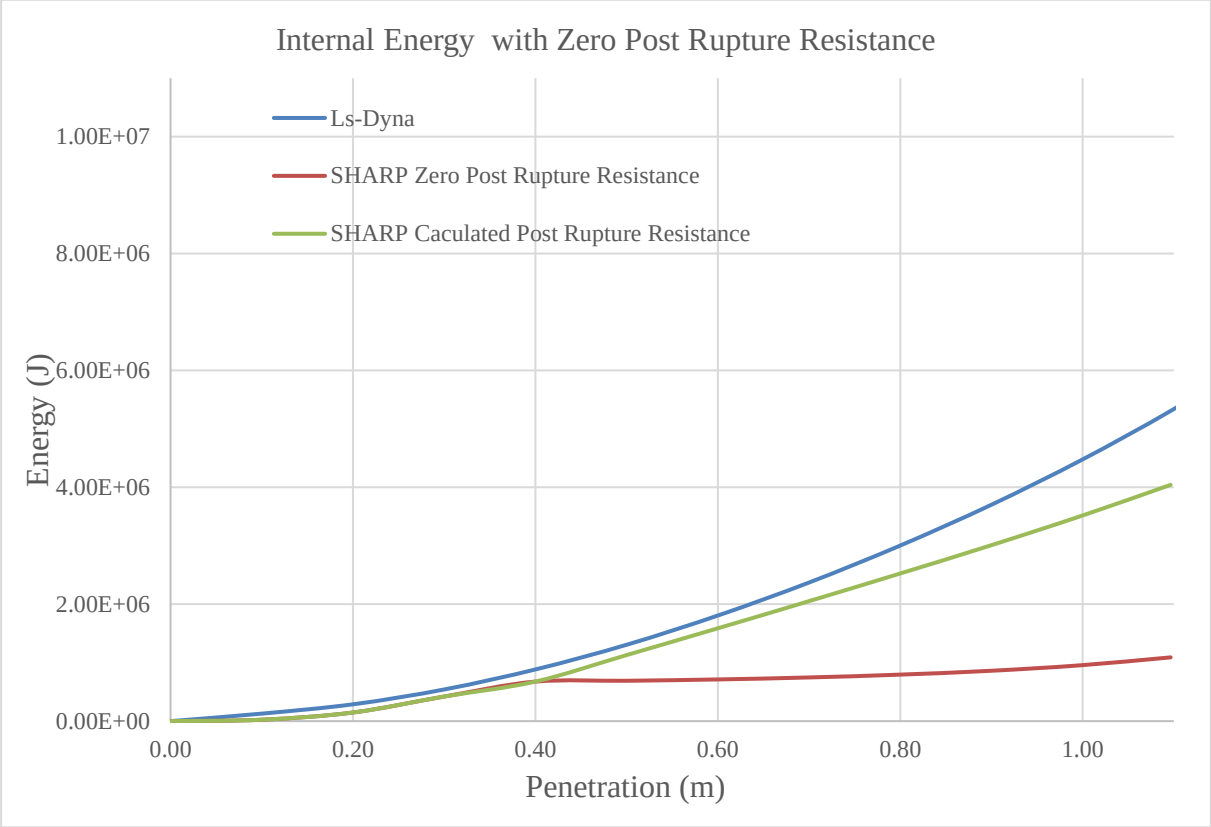

Figure 58 – Total Internal Energy Diagram for Case 2 – Condition 1

In Figure 59, total energy diagram for Case 2 is presented. The influence of the post rupture resistance is noticable after 0.4 m of penetration.

Consequently; for Case – 2, the most effective method is Condition 1 which uses triangular areas and $\delta_{Rupture}$. Case – 3 was not studied, because in that case collapse occurs after 1 m of penetration. Considering both cases, it was decided to use Condition 1 for post rupture resistance calculation code in SHARP. In other words; when the post-rupture resistance will be implemented in SHARP solver, sectional areas of striking ship which represents the non-resisting area of ruptured shell element will be calculated by using triangular shapes. Moreover, $\delta_{Rupture}$ will be used for determining penetrations for each time step. All results can be summarized as in Table 20.

Table 20 – Final Discrepancies with Ls – Dyna Results

	Without P.R.R.	With P.R.R.
Case-1	13%	-9%
Case-2	77%	21%
Case-3	-8%	-8%

In consideration of final results, it can be commented that the proposed formula is effective for calculating post rupture resistance. But it should also be noticed that Case 2 is conservative while the others are not. As the case 2 is concerned, 21% of discrepancy is not a satisfying result, thus the study should be improved.

7.3. Contribution of Different Elements to Total Internal Energy

The difference in total internal energies between SHARP and Ls-Dyna was shown in previous section of this study. In this section, energy contributions of all elements into total internal energy will be demonstrated.

7.3.1. Energy Contributions of Different Elements for Case 1

For Case 1, collision point was just below the deck as shown in Figure 20.

Table 21 - Energy Contributions of Different Elements for Case 1

Parts	**Ls-Dyna**		**Sharp (Wihtout P.R.R)**		**Sharp (Wiht P.R.R)**	
	E (MJ)	**%**	**E (MJ)**	**%**	**E (MJ)**	**%**
Total Energy	5.79		5.03		6.32	
Side Shell	2.45	42.30%	1.18	23.50%	2.47	39.10%
Web Frame	1.81	31.30%	3.80	75.50%	3.80	60.10%
Weather Deck	1.13	19.50%	0.00	0.00%	0.00	0.00%
Stiffners	0.29	5.01%	0.05	1.00%	0.05	0.80%
Others	0.11	1.89%	0.00	0.00%	0.00	0.00%
Penetration	1 m		1 m		1 m	

The most significant point of energy distribution is that; in Ls-Dyna, the energy absorbed by side shell is 2.45 MJ, while in SHARP without post rupture resistance it is 1.18 MJ. But after adding post rupture resistance, it is 2.47 MJ, which is almost same than Ls-Dyna.

It should also be noticed that in SHARP, weather deck does not absorb any energy because it is not impacted. However, some coupling effect between the deformed side shell and the weather deck is observed in LS-DYNA simulation. Indeed, the indentation of the side shell leads to some bending of the weather deck. As a result, some energy is absorbed by the weather deck in LS-DYNA simulation but not in SHARP.

Under these circumstances, the main elements which are resisting to the striking ship are web frames in SHARP. As a consequence, in SHARP, web frames absorb 2.5 times more energy than in Ls-Dyna.

7.3.2. Energy Contributions of Different Elements for Case 2

In this part, different components of total internal energy for Case 2 will be shown. The alignment of both struck and striking ship for this collision scenario can be seen in Figure 24.

Table 22 - Energy Contributions of Different Elements for Case 2

Parts	**Ls-Dyna**		**Sharp (Wihtout P.R.R)**		**Sharp (Wiht P.R.R)**	
	E (MJ)	**%**	**E (MJ)**	**%**	**E (MJ)**	**%**
Total Energy	4.49	1	1.05	1.000	3.52	1.000
Side Shell	2.47	55.00%	0.73	69.50%	3.19	90.70%
Web Frame	1.12	25.00%	0.23	21.80%	0.23	6.50%
Weather Deck	0.18	4.00%	0.00	0.00%	0.00	0.00%
Stiffners	0.45	10.00%	0.09	8.10%	0.09	2.55%
Others	0.27	6.00%	0.01	0.60%	0.01	0.28%
Penetration	1 m		1 m		1 m	

In Table 22, energy contributions of different components are compared. With or without post rupture resistance, the main resistant component to the striking ship is the side shell, both in SHARP and Ls-Dyna. This is expected, because the collision point is far from bottom and deck plates. Therefore, there is no coupling between these parts and side shell. Without post rupture resistance, energy absorbed by side shell is 0.73 MJ which is less than one third of energy absorbed by same component in Ls-Dyna. When post rupture resistance is considered, total value increases up to 3.19 MJ. This increase is relatively high in comparison with the increase

related to Case 1. This is because in this case the main resisting component is the side shell while it was not the case for previous case.

There is another remarkable subject in the table which is the difference in energies absorbed by web frames in Ls-Dyna and SHARP. Because the web frames are not SE1, there is no additional post rupture resistance for them. And in SHARP, energy absorbed by web frames is 0.23 MJ which is less than quarter of the energy absorbed by same elements in Ls-Dyna. The reason for that phenomenon is the lack of coupling effect between web frames in SHARP. In Ls-Dyna, all web frames around the collision area are deformed, in other words they absorb energy. But in SHARP only the ones which are physically in contact with the striking ship bow are deformed.

7.3.3. Energy Contributions of Different Elements for Case 3

For Case 3, post rupture resistance was not applied because the rupture occurs after 1 m of penetration and in scope of ADN it is unnecessary to examine after this value. However, different internal energy components were monitored below in Table 23.

Table 23 - Energy Contributions of Different Elements for Case 3

Parts	**Ls-Dyna**		**Sharp (Wihtout P.R.R)**	
	E (MJ)	**%**	**E (MJ)**	**%**
Total Energy	6.68	1	7.21	1.000
Side Shell	1.40	21.00%	1.92	26.60%
Web Frame	1.54	23.00%	2.61	36.20%
Weather Deck	2.84	42.50%	2.65	36.70%
Stiffners	0.22	3.30%	0.04	0.50%
Others	0.68	10.20%	0.00	0.00%
Penetration	1 m		1 m	

It is clearly seen in Table 23 that when the weather deck is actually active due to the position of the striking bow, SHARP is able to calculate correctly the energy absorbed by that element. The difference between the energy absorbed by weather deck calculated by Ls-Dyna and SHARP is around 6% which can be commented as negligible. For both methods, the main component which resists to the striking ship is the weather deck and that is expected because the striking ship impacts directly that component.

The main difference between SHARP and Ls-Dyna is about web frames. In SHARP, web frames absorbed 2.61 MJ energy while same elements absorbed 1.54 in Ls-Dyna. This can be explained with the same reason than for Case 1. Because, other elements except for the weather deck are not resisting to the striking ship, web frames stand to striking ship's kinetic energy alone. Therefore absorbed energy by those elements are higher in SHARP than Ls-Dyna.

8. CONCLUSION AND RECOMMENDATIONS

In this study, the main deficiencies in SHARP solver were tried to be detected. As it was pointed in a previous study by Sone Oo (2017), it is decided that two main problems are the lack of post rupture resistance and the lack of coupling effect between different elements in same vicinity. Because of time constraints, only the lack of post rupture resistance was studied in this thesis and a new formula was proposed to calculate the resistance force of the elements which were ruptured.

The leading improvement in results of all cases was for Case 2 in which the collision point was around the mid-depth of the struck ship. In that case, the difference about the total internal energies between Ls-Dyna and SHARP was 77% which is far above the acceptable limit. The main work of this master thesis consisted in implementing a new calculation of the post rupture resistance of the struck ship hull. It was shown that, the discrepancy related to Case 2 dropped to 21% which is a significant improvement.

Besides; for the other collision case in which the collision point was just below the weather deck of struck ship and called as Case 1 in this manuscript, the discrepancy between Ls-Dyna and SHARP without post rupture behaviour was 13%. Without any interference that result can be considered as acceptable. But with post rupture resistance, the difference was dropped to 9%. Even that result was non-conservative, the hypothesis can still be commented as effective considering all discrepancies.

In the light of the results of this thesis, new formulation was decided to be implemented in SHARP solver. The coding work is in progress and after implementation, new version will be validated for BV, Nantes. But because of time constraints, the validation of new code could not be shown in this thesis.

After implementing new formulation for post-rupture resistance into SHARP, the most significant deficiency in SHARP will be the lack of coupling effect between the components in same vicinity. It has been shown that because of this insufficiency, some components are not resisting at all or are resisting more than they should.

Furthermore, the drawing interface of the SHARP is not sufficient to model a barge bow. Because of that issue, post rupture behaviour could not be applied for barge bow. Considering the barge bow shape is frequent for inland navigation, that problem can be commented as a remarkable insufficiency.

Finally it should be noted that; including the modelling, setup and processing phases, one Ls-Dyna simulation takes around a week, while using SHARP, the same simulation takes less than half an hour. Considering the required time, expertise and resources, SHARP can be evaluated as a very effective tool. On the other hand still it needs to be slightly improved by integrating the coupling effects.

8.1. Recommendations for Case 1

In Case 1, weather deck of struck ship is not bending and this can be considered as main problem. It is because, there is no coupling between side shell and weather deck. This problem may be solved with the methodology proposed by Buldgen (2013). Besides, the stiffeners in SHARP fails rapidly in comparison with the ones in Ls-Dyna and it should be investigated.

8.2. Recommendations for Case 2

For Case 2, collision point is far from the deck and bottom plates. As a result, the deficiency which is coming from the coupling effect between deck-side and side-bottom, can be neglected. However, this effect is visible for web frames. In Ls-Dyna, all web frames around collision point bend even without direct contact, while only the ones in contact with striking ship are resisting in SHARP. So coupling effect should also be implemented for web frames. Likewise, rapid failure of stiffeners have to be investigated for this case as well.

8.3. Recommendations for Case 3

In this case, failure of the side shell occurs after 1 m of penetration. So post rupture resistance was not implemented. For a future study, a research about rapid failure of stiffeners is advised for this case. Also the energy absorbed by web frames seem to be higher than it should be. The reason behind this behaviour should be studied.

ACKNOWLEDGEMENTS

First of all, I would like to give my intimate thanks to all the professors and mentors who have thought and guided me during all my education life to be in right direction.
Secondly, I would like to express my extensive gratitude to Prof. Hervé Le Sourne, my thesis supervisor at l'Institut Catholique d'Arts et Métiers (ICAM), for sharing his valuable expertise and immense knowledge generously with me.
Thirdly, I would like to state my abiding thanks to Stéphane Paboeuf, another supervisor of mine from Bureau Veritas Marine & Offshore Division in Nantes, who always provided me with precious advices and guidance throughout my internship period.
I would also like to deeply thank all ICAM staff for their openhanded support. In addition, I would like to thank Bureau Veritas teams who welcomed me with open arms and created a warm atmosphere during my internship.
Furthermore, my strong appreciations goes to Prof. Philippe Rigo, the coordinator of the EMSHIP program and also the reviewer of this master thesis, for inviting me to Europe and giving me a chance to take part in this challenging master program.
Also, I would like to say great thanks to my family for supporting me in all manners.
Last but not least, I would like to send my deep gratitudes to all the people, who have directly or indirectly took a part in the development of this thesis. Especially Sone Oo, who studied on SHARP as well and his well-organized work helped me a lot for the thesis study.
This thesis was developed in the frame of the European Master Course in “Integrated Advanced Ship Design” named “EMSHIP” for “European Education in Advanced Ship Design”, Ref.: EMJMD 159652 – Grant Agreement 2015-1687.

Bayram Ozdogan
Thursday, 18 January 2018
Nantes, France

REFERENCES

- A.D.N. Regulations, 2015. *European Agreement concerning the International Carriage of Dangerous Goods by Inland Waterways.* New York and Geneva: United Nations (UN).

- A.D.N. Regulations, 2015. *United Nations Economic Commission for Europe (UNECE)* [online]. Available from: http://www.unece.org/trans/danger/publi/adn/adn_e.html [July 21, 2016].

Besnard, N., 2014. *SHARP 2 V1.0 User Guide.* La Ciotat: PRINCIPIA.

Brown, A.J., Tikka, K., Daidola, J., Lützen, M., Choe, I., Structural Design and Response in Collision and Grounding, *SNAME Transactions 108,* pp.447-473, 2000.

Brown, A.J., Moon, W., Louis, M., 2002. Structural design for crashworthiness in ship collisions, SNAME Annual Meeting T&R 2002 and *SNAME Transactions 110,* pp. 499-512, 2002.

Buldgen, L., Le Sourne, H. and Rigo, P., 2013. A simplified analytical method for estimating the crushing resistance of an inclined ship side. *Marine Structures*, 265-296.

Buldgen, L., Le Sourne, H., Besnard, N. and Rigo, P., 2012. Extension of the super-elements method to the analysis of oblique collision between two ships. *Marine Structures* 29. (pp. 22-57). ELSEVIER.

Calle M, Alves M, 2011. Ship Collision: A Brief Survey, *21st Brazilian Congress of Mechanical Engineering*

Calle M, Alves M 2015. A review-Analysis on Material Failure Modeling in Ship Collision, ELSEVIER.

Donghui Chen, 2000. Simplified ship collision model. Virginia (US)

Eurostat, 2015. *Transport Accident Statistics* [online]. Eurostat Statistics. Available from: http://ec.europa.eu/eurostat/statistics-explained/index.php/Transport_accident_ statistics [June 15, 2016].

Eurostat, 2016. Reference Manual on Inland Waterways Transport Statistics

ITOPF, 2016. *Oil Tanker Spill Statistics 2015* [online]. Statistics - ITOPF. Available from: http://www.itopf.com/fileadmin/data/Documents/Company_Lit/Oil_Spill_Stats_2016.pdf [July 08, 2016]

Jones, N., 1997. *Structural Impact*. Cambridge: Cambridge University Press.

Kitamura, O., 2002. FEM approach to the simulation of collision and grounding damage. *Marine Structures,* 403-428.

Le Sourne, H., Besnard, N., Cheylan, C. and Buannic, N., 2012. A ship collision analysis program based on upper bound solutions and coupled with a large rotational ship movement analysis tool. *Journal of Applied Mathematics.* doi:10.1155/2012/375686

Le Sourne, H., Couty, N., Besnier, F., Kammerer, C. and Legavre, H., 2003. LS-DYNA applications in shipbuilding. *4th European LS-DYNA Users Conference*. Ulm, Germany.

Le Sourne, H., Donner, R., Besnier, F. and Ferry M., 2001. External dynamics of ship–submarine collision. In: Lutzen, M., Simonsen, B.C., Pedersen, P.T. and Jessen, V., editors. Proceedings of *2nd International Conference on Collision and Grounding of Ships;* 2001 July 1–3; Copenhagen, Denmark: Technical University of Denmark. p. 137–144.

Lehmann, E. and Peschmann, J., 2002. Energy absorption by the steel structure of ships in the event of collisions. *Marine Structures,* 15, 429-441.

Lützen, M., Simonsen, B.C. and Pedersen, P.T., 2000. Rapid prediction of damage to struck and striking vessels in a collision event. In *SSC/SNAME/ASNE Symposium.*

Lützen Marie, 2001. *Ship collision damage,* PhD Thesis, Technical University of Denmark.

Minorsky, U.V., 1959. An analysis of ship collisions with reference to nuclear power plants. *Journal of Ship Research*, Vol. 3, Page 1-4.

Naar, H., Kujala, P., Simonsen, B.C. and Ludolphy, H., 2002. Comparison of the crashworthiness of various bottom and side structures. *Marine Structures* 15, 443-460.

OECD, 1993. The Environmental Effects of Freight, Organisation for Economic Co-Operation and Development, Paris

Paboeuf, S., Le Sourne, H., Brochard, K. and Besnard, N., 2015. A damage assessment tool in ship collisions. *RINA Conference, Damaged Ship III*. London, UK.

Paik, J.K., 2007. Practical techniques for finite element modeling to simulate structural crashworthiness in ship collisions and grounding (Part I: Theory). In *Ships and Offshore Structures* (Vol. 2:1, pp. 69-80). doi:10.1533/saos.2006.0148.

Pedersen, P.T. and Zhang, S., 1998. On impact mechanics in ship collisions. Marine Structures, Vol. 11, pp. 429-449.

Pill, I., and Tabri, K., 2011. Finite element simulations of ship collisions: a coupled approach to external dynamics and inner mechanics. In *Ships and Offshore Structures* (Vols. Vol.6:1-2, pp. pp. 59-66). doi:10.1080/17445302.2010.5095857

Ship Structure Committee (SSC), 2002. *Modelling Structural Damage in Ship Collisions.* Report No. 422.

Simonsen, B.C. and Lauridsen, L.P., 2000. Energy absorption and ductile fracture in metal sheets under lateral indentation by a sphere. *International Journal of Impact Engineering*, Vol. 24, 1017-1039.

Simonsen, B.C., 1997. Ship grounding on rocks - I Theory. *Marine Structures*, 10 (7), 519-562.

Simonsen, B.C., and Ocakli, H., 1999. Experiments and theory on deck and girder crushing. (J. Loughlan, Ed.) *Thin-Walled Structures*, Vol. 34, 195-216.

Saul and Svensson, 1982. On the theory of ship collision against bridge piers, [Online] Available from: http://doi.org/10.5169/seals-36657, [27.06.2017]

Sone Oo, P.Y., 2017. *Numerical and analytical simulations of in-shore ship collisions within the scope of A.D.N. Regulations*, Master Thesis, Institut Catholique d'Arts et Métiers, Nantes Campus

Tabri Kristjan, 2010. Dynamics of ship collisions. *Espoo*, Finland

Uzögüten, H. Ö., 2016. *Application of super-element theory to crash-worthiness evaluation within the scope of the A.D.N Regulations*. Master Thesis, West Pomeranian University of Technology, Szczecin.

Vidan, P., Kasum, J. and Misevic, P., 2012. Proposal of measures for increasing the safety level of inland navigation. *Journal of Maritime Research*, Vol IX (1), pp. 57-62.

Wang, G. and Ohtsubo, H., 1997. Deformation of ship plate subjected to very large load. *16th International Conference on Offshore Mechanics and Arctic Engineering (OMAE)*, Vol. 119, pp. 173–180.

Wierzbicki, T., 1995. Concertina tearing of metal plates. *International Journal of Solids and Structures*, Vol. 32 (19), pp. 2923–2943.

Wu, F., Spong, R. and Wang, G., 2004. Using numerical simulation to analyze ship collision. *3rd International Conference on Collision and Grounding of Ships (ICCGS)* (pp. 217-224). Izu, Japan: ICCGS 2004.

Youssef, S.A.M., Kim, Y.S., and Paik, J.K., 2014. Hazard identification and probabilistic scenario selection for ship-ship collision accidents. *The International Journal of Maritime Engineering*, Vol 156, Part A1. doi:10.3940/rina.ijme.2014.a1.277

Zhang, S.M., 1999. *The mechanics of ship collisions*. Ph.D. Thesis, Technical University of Denmark, Department of Naval Architecture and Offshore Engineering.

Zhang, S.M., 2002. Plate tearing and bottom damage in ship grounding. *Marine Structures*, 101-117.